ISSN 2096-7071 (Print)
ISSN 2096-3101 (Online)
CN 10-1629/R1

CHINA CDC WEEKLY

Vol. 7 No. 29 Jul. 18, 2025

中国疾病预防控制中心周报

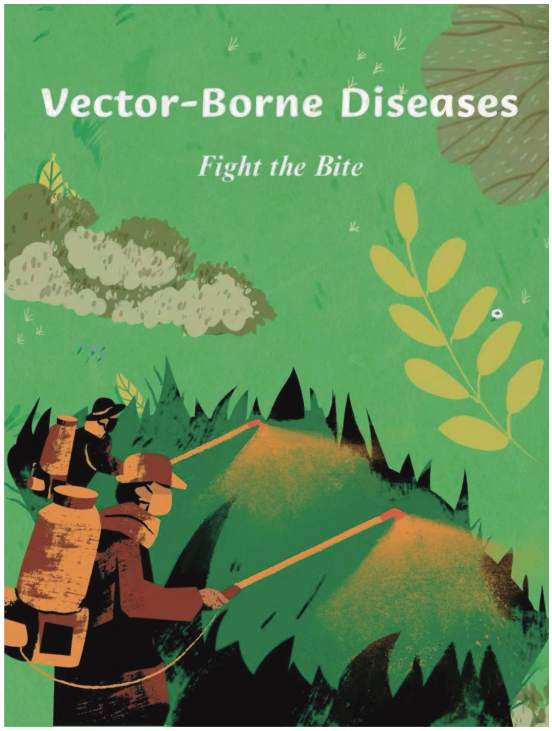

ISSN 2096-7071

Cover Image: adapted from Canva, https://www.canva.cn/.

Vital Surveillances

Notified Vector-Borne Diseases — China, 2005–2024

Qiyong Liu[1,2,#]; Haoqiang Ji[1,2]; Meng Shang[1,2]

ABSTRACT

Introduction: Vector-borne diseases (VBDs) represent a significant category of infectious diseases. Analyzing the epidemiological characteristics of VBDs in China, including their temporal and spatial distributions, provides essential evidence for developing effective prevention and control strategies.

Methods: Data for 14 types of VBDs from 2005 to 2024 were obtained from the China National Infectious Disease Surveillance System. These diseases were categorized as mosquito-borne, tick-borne, rodent-borne, and other VBDs. Using the Mann-Kendall trend test, we analyzed demographic characteristics, spatial distribution, temporal trends, and seasonal patterns of notified cases over the 20-year period.

Results: From 2005 to 2024, a total of 1,129,736 VBD cases were reported in China. Scrub typhus (28.17%), malaria (20.8%), hemorrhagic fever with renal syndrome (HFRS, 18.4%), dengue (12.61%), and schistosomiasis (8.42%) collectively accounted for 88.4% of all cases. Over a 20-year period, mosquito-borne and rodent-borne diseases indicated significant declining trends (P<0.05), while tick-borne and other VBDs demonstrated significant increasing trends (P<0.05). Dengue, scrub typhus, and severe fever with thrombocytopenia syndrome (SFTS) expanded geographically, with annual increases of 10.89, 12.37, and 7.07 reporting cities, respectively. Although diseases such as plague, malaria, and schistosomiasis have been effectively controlled, the incidence of scrub typhus, dengue, HFRS, and SFTS has remained high in recent years.

Conclusions: The burden of VBDs in China remains substantial, with an increasing trend observed over the past 5 years. The rising incidence and geographic expansion of scrub typhus, dengue, and SFTS warrant particular attention from public health authorities.

Vector-borne diseases (VBDs) are caused by bacteria, viruses, or parasites transmitted through vectors such as mosquitoes, ticks, fleas, and rodents (*1*). According to the World Health Organization, 80% of the global population is at risk of at least one VBD, collectively accounting for 17% of the global infectious disease burden (*2*). VBDs cause approximately 700,000 deaths annually, representing a significant global public health threat. China, with its vast territory of approximately 9.6 million square kilometers and population of 1.4 billion, encompasses multiple climate zones and ecological regions that support high biodiversity. This ecological diversity has facilitated the proliferation of numerous disease vectors, resulting in a wide spectrum of VBDs and creating substantial challenges for disease prevention and control efforts (*3*).

Globalization, climate change, and urbanization have substantially altered vector habitats, potentially expanding or shifting their geographical distribution (*4*). These environmental changes facilitate pathogen transmission to human populations, increasing the risk of emerging and reemerging infectious diseases, including VBDs. Over the past two decades, China has identified new VBDs such as severe fever with thrombocytopenia syndrome (SFTS) and Zika virus disease, while established diseases like dengue and hemorrhagic fever with renal syndrome (HFRS) have caused recurrent outbreaks (*5*–*6*). These infectious diseases pose significant threats to social stability, economic development, and public health in China. Therefore, exploring disease patterns and transmission trends is essential for implementing effective VBD control and prevention strategies.

METHODS

This study analyzed data from 14 VBDs recorded in the China national infectious disease surveillance system from 2005 to 2024. We categorized these diseases into four groups: mosquito-borne diseases (dengue, malaria, Japanese encephalitis, Zika virus disease, and filariasis), tick-borne diseases [severe fever

with thrombocytopenia syndrome (SFTS) and tick-borne encephalitis], rodent-borne diseases [hemorrhagic fever with renal syndrome (HFRS), leptospirosis, and plague], and others (scrub typhus, schistosomiasis, typhus group rickettsiosis, and leishmaniasis). After excluding 32,102 suspected cases, we analyzed the spatial distribution, temporal trends, and demographic characteristics of these four VBD categories over the 20-year period. We used analysis of variance to examine differences in continuous variables between groups, Chi-square tests to analyze differences in categorical variables, and the Mann-Kendall trend test to evaluate temporal trends in disease incidence. All data processing and statistical analyses were performed using R (version 4.2.2; The R Foundation for Statistical Computing, Vienna, Austria).

RESULTS

From 2005 to 2024, China reported a total of 1,129,736 cases of VBDs (annual incidence rate of 4.13 per 100,000), with 6,096 deaths (Table 1). Scrub typhus accounted for the highest number of cases (318,258), followed by malaria (235,033), HFRS (207,850), and dengue (142,422). Tick-borne diseases exhibited the highest cumulative fatality rate (4.33%) during this period. Among individual diseases, plague had the highest case fatality rate (38.33%), followed by Japanese encephalitis (4.9%) and SFTS (4.79%). The mean age of all VBD cases was 43.85 years (SD: 20.04), with tick-borne disease cases having the highest mean age of 61.51 years (SD: 13.66). Males comprised a higher proportion of cases in all disease categories except tick-borne diseases. Across all VBD types, farmers represented a significantly higher proportion of cases compared to individuals in other occupations (Table 2, all $P<0.05$).

Mosquito-borne diseases, primarily malaria (56.39%) and dengue (34.17%), are predominantly distributed in the southern regions of China (Figure 1). Tick-borne diseases, mainly SFTS (89.07%), are concentrated in Central and Eastern China. Rodent-borne diseases, predominantly HFRS (95.53%), are primarily found in Northeast China and along the middle and lower reaches of the Yangtze and Yellow Rivers. Other vector-borne diseases, chiefly scrub typhus (69.63%), are mainly distributed across Southwest and South China regions. Notably, dengue,

TABLE 1. The incidence and fatality of VBDs in China from 2005 to 2024.

Disease	Cases (No.)	Cumulative incidence (per 100,000)	Death (No.)	Fatality rate (%)
VBD	1,129,736	82.60	6,096	0.54
Mosquito-borne disease	416,813	30.47	2,292	0.55
Dengue	142,422	10.41	14	0.01
Malaria	235,033	17.18	350	0.15
Japanese encephalitis	39,303	2.87	1,927	4.90
Zika virus disease	39	–	0	0.00
Filariasis	16	–	1	6.25
Tick-borne disease	38,241	2.80	1,656	4.33
SFTS	34,063	2.49	1,631	4.79
Tick-borne encephalitis	4,178	0.31	25	0.60
Rodent-borne diseases	217,579	15.91	2,001	0.92
HFRS	207,850	15.20	1,806	0.87
Leptospirosis	9,669	0.71	172	1.78
Plague	60	–	23	38.33
Others	457,103	33.42	147	0.03
Scrub typhus	318,258	23.27	108	0.03
Schistosomias	95,093	6.95	14	0.01
Typhus group rickettsiosis	37,673	2.75	6	0.02
Leishmaniasis	6,079	0.44	19	0.31

Abbreviation: VBD=vector-borne disease; No.=number; HFRS=hemorrhagic fever with renal syndrome; SFTS=severe fever with thrombocytopenia syndrome.

TABLE 2. The Characteristics of cases with VBDs in China from 2005 to 2024.

Characteristics	Mosquito-borne disease	Tick-borne disease	Rodent-borne diseases	Others	*P*
Age [mean (SD)]	36.24 (20.02)	61.51 (13.66)	45.31 (15.80)	48.61 (19.75)	<0.001
Gender (%)					
Female	152,948 (36.69)	19,385 (50.69)	56,169 (25.82)	224,737 (49.17)	<0.001
Male	263,865 (63.31)	18,856 (49.31)	161,410 (74.18)	232,366 (50.83)	
Occupation (%)					
Children	33,522 (8.04)	71 (0.19)	884 (0.41)	26,912 (5.89)	<0.001
Service industry	25,318 (6.07)	187 (0.49)	4,689 (2.16)	4,240 (0.93)	
Farmer	165,919 (39.81)	29,944 (78.30)	147,420 (67.75)	339,774 (74.33)	
Unemployed	33,686 (8.08)	4,039 (10.56)	16,332 (7.51)	21,626 (4.73)	
Pupil	51,199 (12.28)	157 (0.41)	9,734 (4.47)	22,496 (4.92)	
Staff of public institutions	12,364 (2.97)	323 (0.84)	5,845 (2.69)	6,474 (1.42)	
Others	94,805 (22.75)	3,520 (9.20)	32,675 (15.02)	35,581 (7.78)	

Abbreviation: VBD=vector-borne disease; SD=standard deviation.

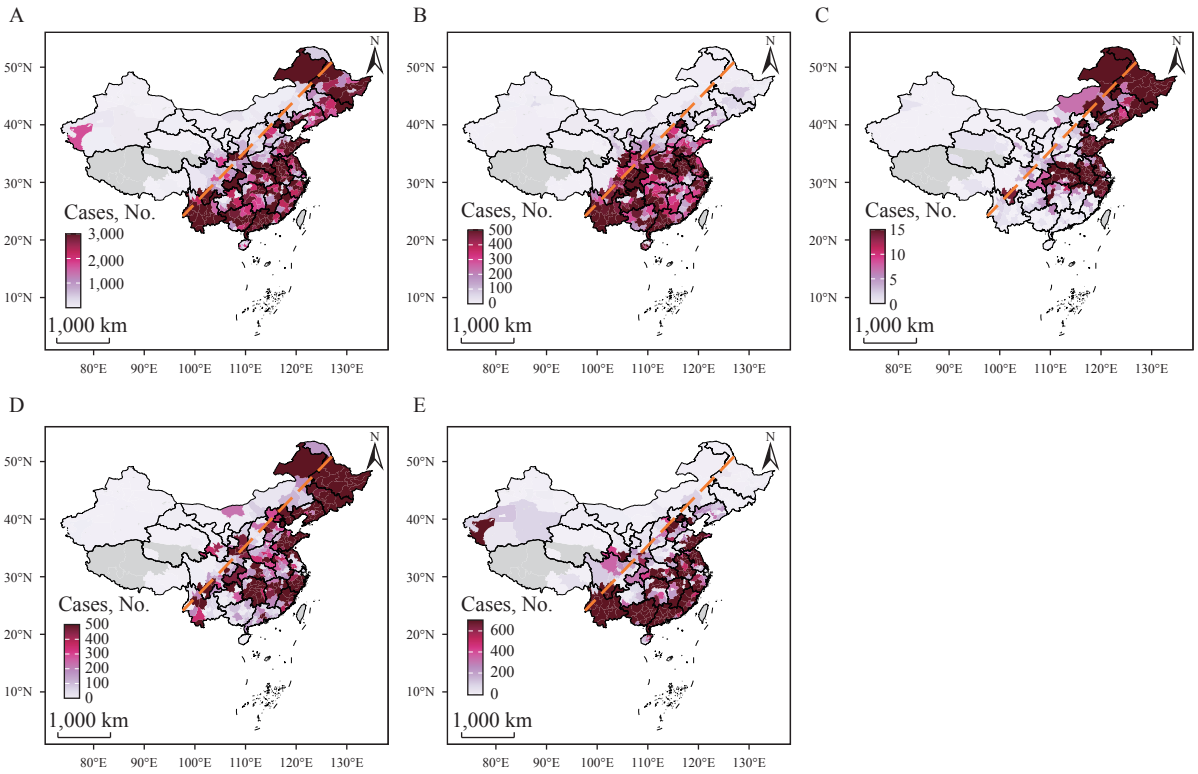

FIGURE 1. Spatial distribution of VBDs in China from 2005 to 2024. (A) VBDs; (B) Mosquito-borne diseases; (C) Tick-borne diseases; (D) Rodent-borne disease; (E) Other diseases.
Abbreviation: VBD=vector-borne disease; No.=number.
Map approval number: GS 京 (2025)0996 号.

scrub typhus, and SFTS have demonstrated annual increases in geographic spread, with reported cases expanding to 10.89, 12.37, and 7.07 more cities each year, respectively (Supplementary Figures S1–S3, available at https://weekly.chinacdc.cn/).

From 2005 to 2024, the incidence of VBDs in China has exhibited a fluctuating pattern with three distinct peaks occurring in 2006, 2014, and 2024 (P=0.721, Figures 2A and 2C). Mosquito-borne and rodent-borne diseases showed significant declining trends, while tick-borne diseases and other VBDs demonstrated significant increasing trends (all P<0.05).

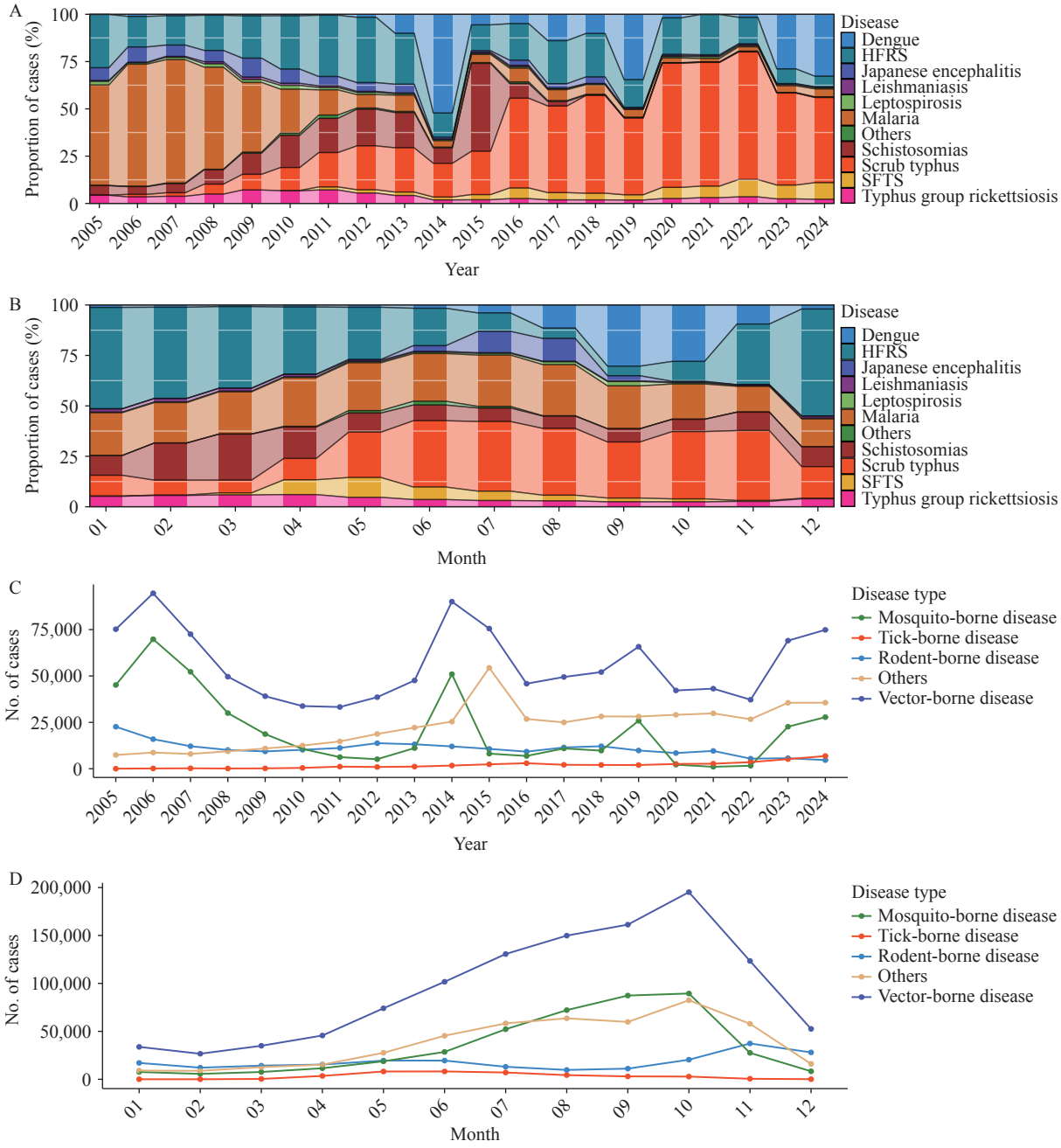

FIGURE 2. The trends in incidence and seasonal characteristics of VBDs in Mainland China from 2005 to 2024. (A) Annual case distribution (%) of vector-borne diseases by disease; (B) Monthly case distribution (%) of vector-borne diseases by disease; (C) Annual reported cases of VBDs by vector category; (D) Monthly reported cases of vector-borne diseases by vector category.
Abbreviation: VBD=vector-borne disease; No.=number; HFRS=hemorrhagic fever with renal syndrome; SFTS=severe fever with thrombocytopenia syndrome.

The first two peaks were primarily attributed to outbreaks of malaria and dengue, while the 2024 peak resulted mainly from increased scrub typhus and dengue cases. From 2004 to 2014, malaria and HFRS cases constituted a higher proportion of VBDs in China, whereas from 2014 to 2024, dengue, SFTS, and scrub typhus became more prevalent. Mann-Kendall trend analysis revealed that rodent-borne diseases (HFRS, leptospirosis), malaria, Japanese encephalitis, schistosomiasis, and typhus group rickettsiosis have shown significant declining trends, while SFTS, dengue, and scrub typhus have demonstrated significant increasing trends (all $P<0.05$). Additionally, VBDs exhibit distinct seasonal

distribution patterns (Figure 2B and 2D). HFRS displays bimodal annual incidence peaks, dengue cases peak from June to October, and SFTS cases peak from May to August. Scrub typhus shows a higher proportion of cases from June to November.

DISCUSSION

From 2005 to 2024, VBDs in China exhibited a fluctuating trend, with previous studies documenting a fluctuating decline from 2005 to 2020 (*1*), followed by a notable increase in recent years. This recent upward trend necessitates strengthened preventive measures to mitigate further case increases in 2025. Over the past two decades, high-threat diseases such as plague, HFRS, malaria, and Japanese encephalitis have been generally controlled. However, dengue has emerged as a significant mosquito-borne disease, replacing malaria and Japanese encephalitis as a major public health threat in China. Additionally, SFTS, a newly emerging tick-borne disease, presents a high fatality rate that warrants urgent attention. While rodent-borne diseases have generally been controlled, HFRS cases remain at concerning levels. Therefore, China should intensify measures to prevent the spread of dengue and SFTS, while also focusing on the prevention of key VBDs and emerging infectious diseases to avoid outbreaks.

In the context of global warming and urbanization, preventing mosquito-borne disease outbreaks and controlling their northward spread should be prioritized (*7*). SFTS, as an emerging infectious disease, is spreading rapidly, necessitating enhanced research and prevention efforts to identify factors driving its spread and prevent further expansion (*8*). Scrub typhus, which has become a major VBD in recent years in China, is primarily prevalent in southern regions and manifests a trend of further geographical expansion (*9*). Simultaneously, flea monitoring should be strengthened to prevent potential plague outbreaks in endemic areas. In high-risk regions, vaccination efforts should be intensified to prevent HFRS outbreaks, with particular attention to outbreaks triggered by extreme events such as floods (*10*). Additionally, prevention and control measures for dengue and scrub typhus should be strengthened before summer and autumn, while HFRS prevention should be enhanced before winter and spring. Currently, the epidemiological trends of VBDs in China pose a significant health threat to the population, especially among elderly farmers who are particularly vulnerable due to their poor health status and low economic resources. Tailored interventions should be developed, including community health education, free vaccination programs, and early warning systems to reduce social inequities.

In summary, a substantial gap remains between China's current VBD control efforts and the goals proposed by the World Health Organization. Therefore, intensified efforts are needed to prevent the continued increase in VBD cases in and beyond 2025, especially for the control and prevention of dengue, scrub typhus, and SFTS. Additionally, we need to strengthen monitoring and prevention of outbreaks of emerging infectious diseases and those not legally required to be reported. We should also promote patriotic health campaigns, implement integrated vector management, and ensure sustainable vector control to effectively mitigate VBD risks (*11*). This study has several limitations. First, some VBDs, such as Yellow Fever, Lyme disease, and bartonellosis, were not included in the disease notification system and therefore were not analyzed. Second, there may be cases where individuals did not seek medical treatment and thus were not reported, potentially resulting in a higher actual disease burden than reflected in this study. Finally, the 20-year epidemic trend of VBDs may have been influenced by monitoring capabilities, the COVID-19 pandemic, and various natural social policy events.

Conflicts of interest: No conflicts of interest.

Acknowledgments: The Chinese Center for Disease Control and Prevention for their software support and administrative assistance.

Funding: Supported by the consultancy project (2023-JB-12) from the Chinese Academy of Engineering (CAE) and the Key Program of the National Natural Science Foundation of China (GRANT32090023).

doi: 10.46234/ccdcw2025.162

[#] Corresponding author: Qiyong Liu, liuqiyong@icdc.cn.

[1] National Key Laboratory of Intelligent Tracking and Forecasting for Infectious Diseases, National Institute for Communicable Disease Control and Prevention, Chinese Center for Disease Control and Prevention, Beijing, China; [2] Department of Vector Control, School of Public Health, Cheeloo College of Medicine, Shandong University, Jinan City, Shandong Province, China.

Submitted: January 21, 2025
Accepted: April 15, 2025
Issued: July 18, 2025

REFERENCES

1. Liu QY. Reported cases of vector-borne diseases in China, 2005-2020: epidemic trend, challenges in prevention and control, and related coping strategies. Chin J Vector Biol Control 2022;33(1):1 – 7. https://doi.org/10.11853/j.issn.1003.8280.2022.01.001.
2. World Health Organization. Global vector control response 2017-2030: a strategic approach to tackle vector-borne diseases. Geneva: World Health Organization; 2017. https://iris.who.int/bitstream/handle/10665/259002/WHO-HTM-GVCR-2017.01-eng.pdf?sequence=1.
3. Liu QY. Epidemic profile of vector-borne diseases and vector control strategies in the new era. Chin J Vector Biol Control 2019;30(1):1 – 6, 11. https://doi.org/10.11853/j.issn.1003.8280.2019.01.001.
4. Liu QY, Xu WB, Lu S, Jiang JF, Zhou JP, Shao ZJ, et al. Landscape of emerging and re-emerging infectious diseases in China: impact of ecology, climate, and behavior. Front Med 2018;12(1):3 – 22. https://doi.org/10.1007/s11684-017-0605-9.
5. Liu QY, Gao Y. Reported vector-borne diseases - China, 2018. China CDC Wkly 2020;2(14):219-24. https://pubmed.ncbi.nlm.nih.gov/34594627/.
6. Liu QY. Dengue fever in China: new epidemical trend, challenges and strategies for prevention and control. Chin J Vector Biol Control 2020;31(1):1 – 6. https://doi.org/10.11853/j.issn.1003.8280.2020.01.001.
7. Li CX, Liu Z, Li W, Lin YX, Hou LY, Niu SY, et al. Projecting future risk of dengue related to hydrometeorological conditions in mainland China under climate change scenarios: a modelling study. Lancet Planet Health 2023;7(5):e397 – 406. https://doi.org/10.1016/S2542-5196(23)00051-7.
8. Sun JM, Lu L, Wu HX, Yang J, Ren JP, Liu QY. The changing epidemiological characteristics of severe fever with thrombocytopenia syndrome in China, 2011-2016. Sci Rep 2017;7(1):9236. https://doi.org/10.1038/s41598-017-08042-6.
9. Yue YJ, Ren DS, Liu XB, Wang YJ, Liu QY, Li GC. Spatio-temporal patterns of scrub typhus in mainland China, 2006-2017. PLoS Negl Trop Dis 2019;13(12):e0007916. https://doi.org/10.1371/journal.pntd.0007916.
10. Ji HQ, Li K, Shang M, Wang ZX, Liu QY. The 2016 severe floods and incidence of hemorrhagic fever with renal syndrome in the Yangtze River basin. JAMA Netw Open 2024;7(8):e2429682. https://doi.org/10.1001/jamanetworkopen.2024.29682.
11. Liu QY. Sustainable vector management strategy and practice: achievements in vector-borne diseases control in new China in the past seventy years. Chin J Vector Biol Control 2019;30(4):361 – 6. https://doi.org/10.11853/j.issn.1003.8280.2019.04.001.

SUPPLEMENTARY MATERIAL

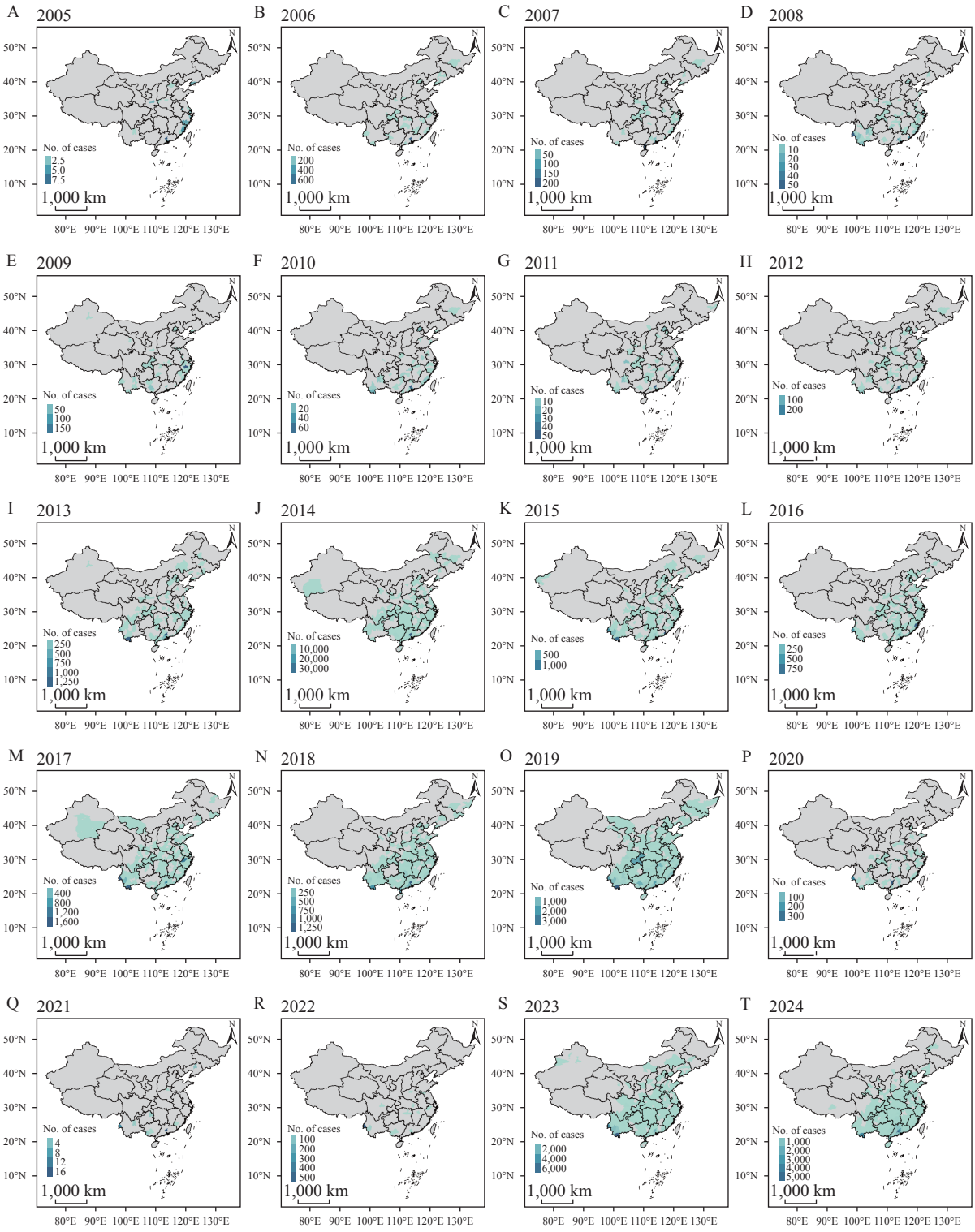

SUPPLEMENTARY FIGURE S1. The spatial diffusion pattern of dengue in China from 2005 to 2024. (A)–(T) 2005–2024.
Abbreviation: No.=number.
Map approval number: GS 京 (2025)0996 号.

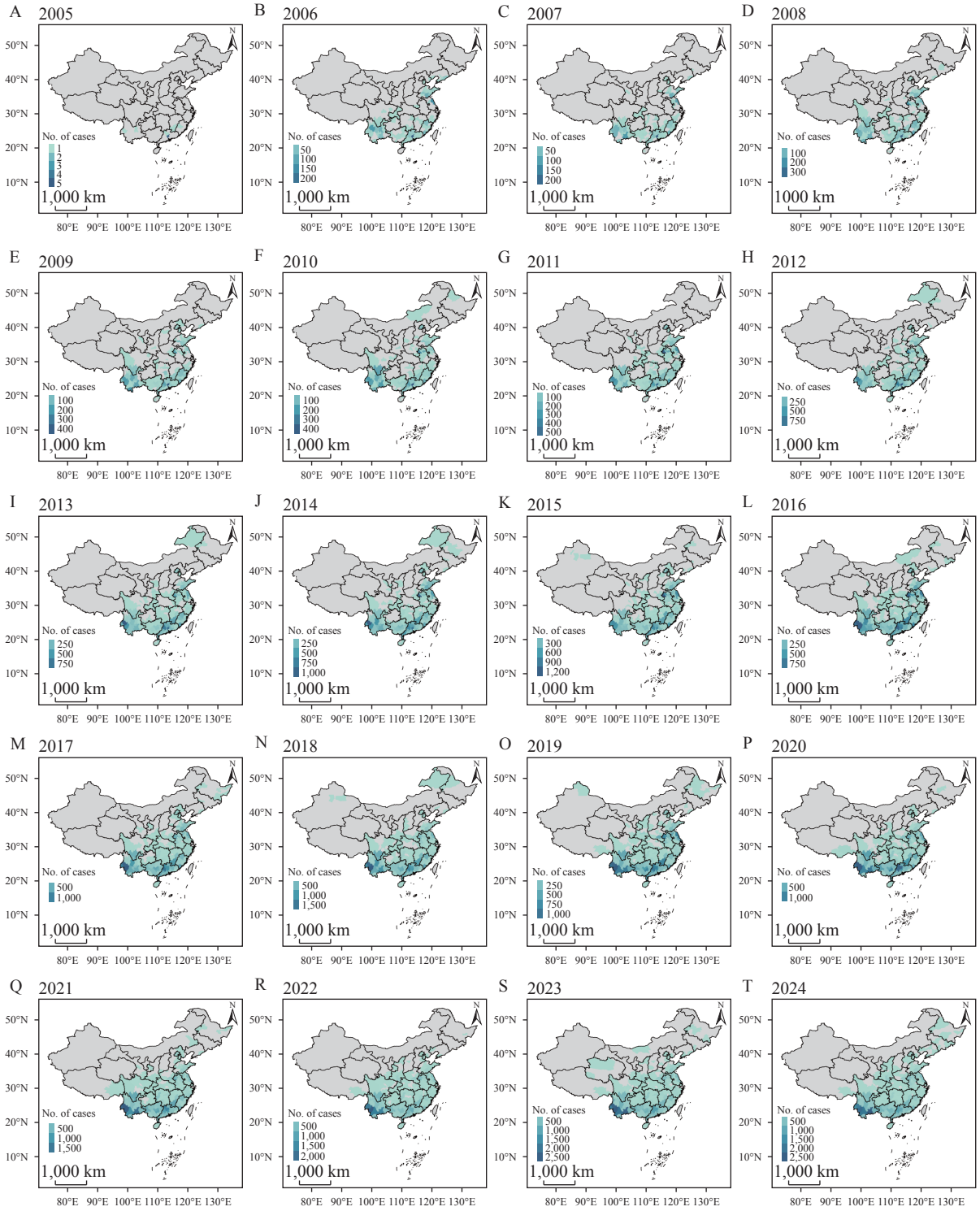

SUPPLEMENTARY FIGURE S2. The spatial diffusion pattern of scrub typhus in China from 2005 to 2024. (A)−(T) 2005−2024.
Abbreviation: No.=number.
Map approval number: GS 京 (2025)0996 号.

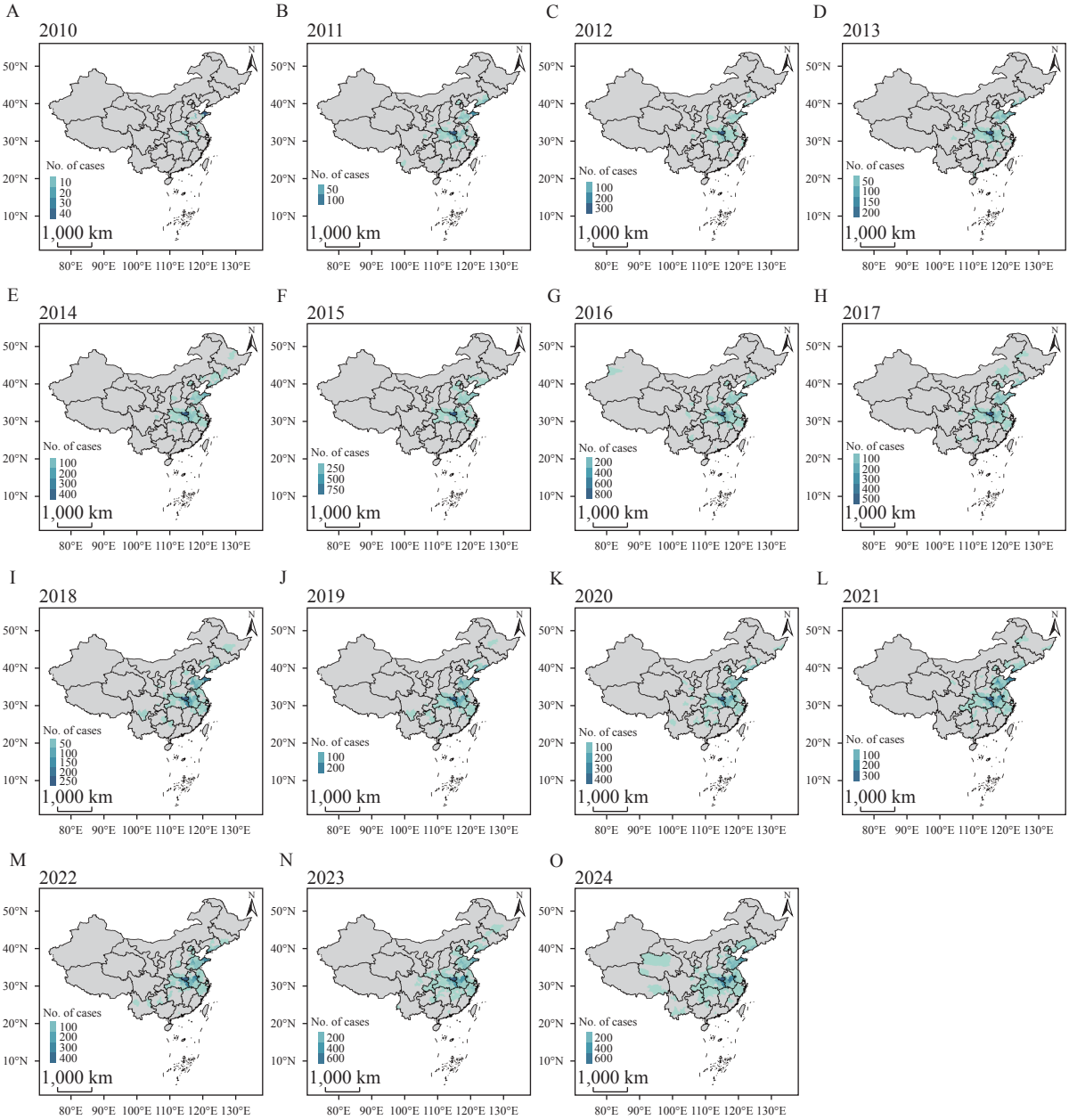

SUPPLEMENTARY FIGURE S3. The spatial diffusion pattern of SFTS in China from 2010 to 2024. (A)−(T) 2010–2024.
Abbreviation: No.=number; SFTS=severe fever with thrombocytopenia syndrome.
Map approval number: GS 京 (2025)0996 号.

Vital Surveillances

A Comprehensive Analysis and Forecast of Rabies Epidemic and Elimination Challenges — China, 2005–2023

Na Zhang[1]; Xiaonuo Xu[1]; Minghui Zhang[1]; Yuan Xie[1]; Pengcheng Yu[1]; Shuqing Liu[1]; Qian Liu[1]; Xiaoyan Tao[1,#]; Wuyang Zhu[1,#]

ABSTRACT

Introduction: The 2030 global target for eliminating dog-mediated human rabies, jointly proposed by the World Health Organization (WHO) and other international organizations, presents significant challenges for China. This study analyzes epidemiological trends (2005–2023), forecasts future case numbers, and compares China's progress with elimination strategies from the United States, Japan, and Brazil to optimize national rabies prevention and control approaches.

Methods: Descriptive statistics were used to analyze the spatiotemporal distribution of human rabies cases across China. The seasonal autoregressive integrated moving average (SARIMA) model was employed to forecast cases for the next two years, with the optimal model selected based on indicators, including the Akaike information criterion.

Results: 24,566 human rabies cases were reported in China from 2005 to 2023. Over these 19 years, rabies prevalence shifted from southeastern to northwestern regions. Provincial trends varied significantly: 14 provincial-level administrative divisions, including Beijing, Tianjin, and Shanghai, achieved zero cases; Shandong, Shanxi, and Chongqing experienced a resurgence; Guangxi, Henan, Hunan, and Anhui maintained high endemic levels; while other regions showed a steady decline. The SARIMA $(0,1,2)(2,1,1)_{12}$ model forecasts 65 cases by 2025, substantially exceeding international case levels during comparable elimination phases.

Conclusions: To achieve the 2030 rabies elimination goal in China, implementing a comprehensive, large-scale dog vaccination strategy is essential within the remaining timeframe.

Rabies is an acute and lethal zoonotic disease that affects the central nervous system of all warm-blooded animals (*1*). The primary transmission route is from infected canines to humans, with nearly 100% mortality once clinical symptoms appear (*2*). Currently, human rabies causes an estimated 59,000 deaths annually across more than 150 countries, predominantly in low and middle-income regions of Asia and Africa (*3*). In 2015, the World Health Organization and other international organizations established a global target to eliminate dog-mediated human rabies by 2030 (*4*). Several regions have already achieved this goal, including Western Europe, Canada, the USA, Japan, and 28 Latin American countries. Various Asian and African countries have made significant progress in reducing human rabies cases (*5*). In China, human rabies caused over 1,000 deaths annually from 2002 to 2004, representing the highest mortality among notifiable communicable diseases during that period (*6*). Since establishing sentinel surveillance in 2005, China has implemented comprehensive control measures, including policies and regulations for rabies prevention, improved surveillance and management systems, and the development of effective vaccines and treatments (*7*). These efforts have resulted in a consistent annual decrease in cases beginning in 2008, demonstrating substantial progress in epidemic control (*8*). Given these favorable prevention and control outcomes, the question of how much further case numbers can decrease in the next two years emerges. This study aims to analyze the epidemiological characteristics and trends of human rabies in China to provide a scientific foundation for implementing and refining rabies control strategies.

METHODS

Data Sources and Collection

Human rabies case data (2005–2023) were retrieved from the National Notifiable Disease Reporting System and provided by the China CDC.

Data Analysis

Microsoft Excel 2021 (Microsoft Corporation, Redmond, WA, USA) was used to organize the human rabies data. Counted data were presented as frequency or component ratio. Categorical data were analyzed using a chi-squared (χ^2) test and a one-way analysis of variance. Implementation of the SARIMA model involved four steps: model identification, parameter estimation, model diagnosis, and model prediction.

All statistical analyses were conducted using R software (https://www.r-project.org/). A *P* value <0.05 was considered statistically significant. Spatial distribution maps were generated with ArcGIS software (version 10.8; ESRI Inc., Redlands, CA, USA).

Comparison of Cases Among Countries

Rabies case data from 5, 10, and 15 years preceding elimination in three countries (USA, Japan, and Brazil) were compared with projected cases in China.

RESULTS

Overall Epidemic Trend

24,566 human rabies cases were reported in China from 2005 to 2023, with an annual average of 1,293 cases and an incidence rate of 0.096 cases per 100,000 persons. Since peaking in 2008, cases have steadily decreased to only 120 in 2023, the lowest level recorded since 1951 (Figure 1A). The geographic scope of the epidemic has also contracted significantly, with affected provincial-level administrative divisions (PLADs) fluctuating between a maximum of 29 in 2013 and a minimum of 16 in 2022. The number of affected counties decreased dramatically from 997 in 2007 to 101 in 2023, indicating a transition to a sporadic epidemiological pattern.

Regional Distribution

Regional distribution of cumulative cases From 2005 to 2023, human rabies cases were reported in all PLADs of China, with 55.61% (13,660/24,566) of cases occurring in 11 southeastern PLADs (Fujian, Guangdong, Hainan, Jiangxi, Zhejiang, Jiangsu, Shanghai, Guangxi, Hunan, Hubei, and Anhui).

Changes in rabies epidemiology across PLADs The spatial distribution of human rabies from 2005 to 2023 can be divided into three distinct phases: 2005–2007, 2008–2014, and 2015–2023. During 2005–2007, five PLADs (Xizang, Qinghai, Gansu, Ningxia, and Liaoning) reported no cases. In 2008–2014, the number of cases further decreased, with Xizang and Jilin reporting no cases. By 2015–2023, rabies cases were reported throughout the country, with sporadic events occurring in previously rabies-free regions.

Based on changes in the proportion of cases relative to the total number reported, PLADs can be categorized into four zones: no cases, declining epidemic, re-emergent epidemic, and high incidence (top five reported cases) (Table 1). From 2005 to 2023, 14 PLADs achieved zero cases, with Liaoning, Jilin, Heilongjiang, Xinjiang, Qinghai, Xizang, Shanghai, Beijing, and Tianjin, reporting no cases for three or more consecutive years, and Hainan, Fujian, Inner Mongolia, Gansu, and Ningxia for two consecutive years. Shandong (2020), Shanxi (2021), and Chongqing (2020) also achieved zero cases in the past but experienced a case resurgence from 2021 to 2023. Hunan, Henan, Guangxi, and Anhui maintained high prevalence, with Henan showing a significant increase in case proportion, accounting for more than 10% in 2016, and rising to 28.33% in 2023. Cases in Guangxi showed a declining trend, even though the PLAD ranked among the top three for 16 years. Hunan remained among the top three PLADs for 68.42% (13/19) of the study period, ranking first from 2016 to 2022. The percentage of cases in Anhui steadily increased, and the PLAD has consistently ranked in the top four since 2019.

Time Distribution

Human rabies cases occur year-round, with peaks between June and November, typically in August (Supplementary Figure S1, available at https://weekly.chinacdc.cn/). Throughout the 19-year study period, August was the peak month for nine years and October for seven years. On average, August accounted for 10.93% of cases [95% confidence interval (*CI*): 9.34%, 12.52%], while February had the lowest proportion at 5.60% (95% *CI*: 3.01%, 7.19%). The χ^2 test showed no significant difference in monthly rabies incidence across years (*P*>0.05). Notably, following the peak in 2007 and particularly since 2012, the seasonal pattern has become less pronounced as annual case numbers have continued to decline.

Demographic Features

The incidence of human rabies in China varies by sex, age, and occupation. The overall male-to-female ratio was 2.33:1 (17,196:7,370), with no significant

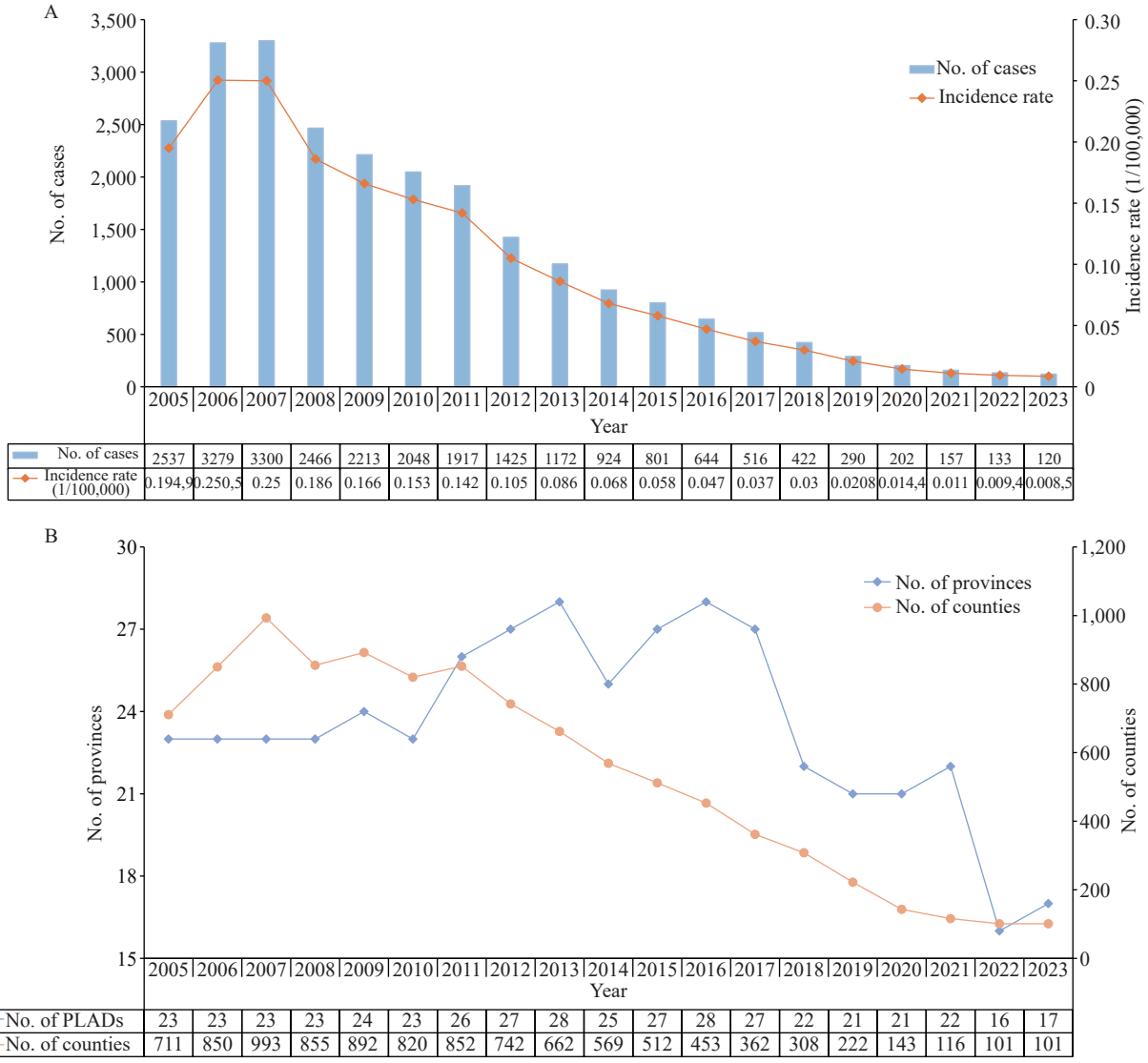

	2005	2006	2007	2008	2009	2010	2011	2012	2013	2014	2015	2016	2017	2018	2019	2020	2021	2022	2023
No. of cases	2537	3279	3300	2466	2213	2048	1917	1425	1172	924	801	644	516	422	290	202	157	133	120
Incidence rate (1/100,000)	0.194,9	0.250,5	0.25	0.186	0.166	0.153	0.142	0.105	0.086	0.068	0.058	0.047	0.037	0.03	0.0208	0.014,4	0.011	0.009,4	0.008,5
No. of PLADs	23	23	23	23	24	23	26	27	28	25	27	28	27	22	21	21	22	16	17
No. of counties	711	850	993	855	892	820	852	742	662	569	512	453	362	308	222	143	116	101	101

FIGURE 1. Time series analyses of human rabies cases in China, 2005–2023. (A) Annual cases and incidence; (B) Affected areas.
Abbreviation: PLAD=provincial-level administrative division.

TABLE 1. Rabies epidemic in China from 2005 to 2023.

Epidemic zone	Provincial-level administrative divisions	Proportion changes (%)	Counting
No. of cases	Liaoning, Jilin, Heilongjiang, Xinjiang, Qinghai, Xizang, Shanghai, Beijing, Tianjin, Hainan, Fujian, Inner Mongolia, Gansu, Ningxia	0–1.74	14
Decline	Yunnan, Jiangsu, Guangdong, Sichuan, Hebei, Shaanxi, Zhejiang, Guizhou, Jiangxi, Hubei	0.03–19.55	10
Re-emergent	Shandong, Shanxi, Chongqing	0–7.02	3
High Prevalence	Guangxi, Hunan, Henan, Anhui	1.58–31.85	4

annual variation (P>0.05). Significant differences were observed across age groups (P<0.001), with individuals aged 50–60 being the most affected (Supplementary Figure S2A, available at https://weekly.chinacdc.cn/). Statistically significant differences in incidence rates were also observed across occupational groups, with farmers being the most affected (68.4%), followed by students (12.13%) and children (6.46%) (Supplementary Figure S2B).

SARIMA Model Prediction

Using monthly human rabies case data from China (2005–2023), we established and plotted a time series

(Figure 2A). The seasonal-trend decomposition revealed distinct seasonality with peaks from August to October, indicating a nonstationary series (Figure 2B). We applied a log transformation with first-order regular and seasonal differencing (d=1, D=1), which effectively eliminated the seasonal pattern. The augmented Dickey–Fuller (ADF) test confirmed that the differential series was stationary (ADF=−5.9811, P<0.001). The autocorrelation function (ACF) and partial autocorrelation function (PACF) plots suggested parameters p, P, q, and Q should be set between 0 and 2 (Supplementary Figure S3A–B, available at https://weekly.chinacdc.cn/). We selected the SARIMA $(0,1,2)(2,1,1)_{12}$ model based on optimal Akaike information criterion (AIC), Bayesian information criterion (BIC), and log-likelihood values (Supplementary Table S1, available at https://weekly.chinacdc.cn/), which demonstrated statistically significant parameters (Supplementary Table S2, available at https://weekly.chinacdc.cn/). The Ljung–Box test confirmed the residuals were white noise (χ^2=0.331, P=0.565), while the ACF and PACF plots indicated they were random and independent (Supplementary Figure S3C–D).

Our predictions showed a continued decline in rabies cases, with an estimated 83 cases in 2024 and 65 cases in 2025 (Supplementary Table S3, available at https://weekly.chinacdc.cn/). The actual values closely matched the fitted values, with all predictions falling within the 95% *CI*, thereby validating the model's accuracy and reliability (Figure 3). Notably, actual incidence may be influenced by factors such as control measures, changes in public health policies, and unforeseen circumstances, which introduce uncertainties into the predictions.

Comparison of Elimination Progress

Projecting toward the 2030 elimination target, human rabies cases in China are expected to decrease to 65 by 2025. In comparison, the United States eliminated human rabies in 2007, reporting only 2, 3, and 2 cases in the 15, 10, and 5 years preceding elimination, respectively (*9*). Japan achieved elimination in 1956, with fewer than 10 cases reported during both the 5-year and 10-year periods prior to elimination (*10*). Brazil eliminated rabies in 2016, reporting 23, 5, and 2 cases at 15, 10, and 5 years before elimination, respectively (*11*) (Table 2).

DISCUSSION

Rabies remains endemic in China, but significant progress has been made since 2005 due to comprehensive monitoring and control measures (*8*).

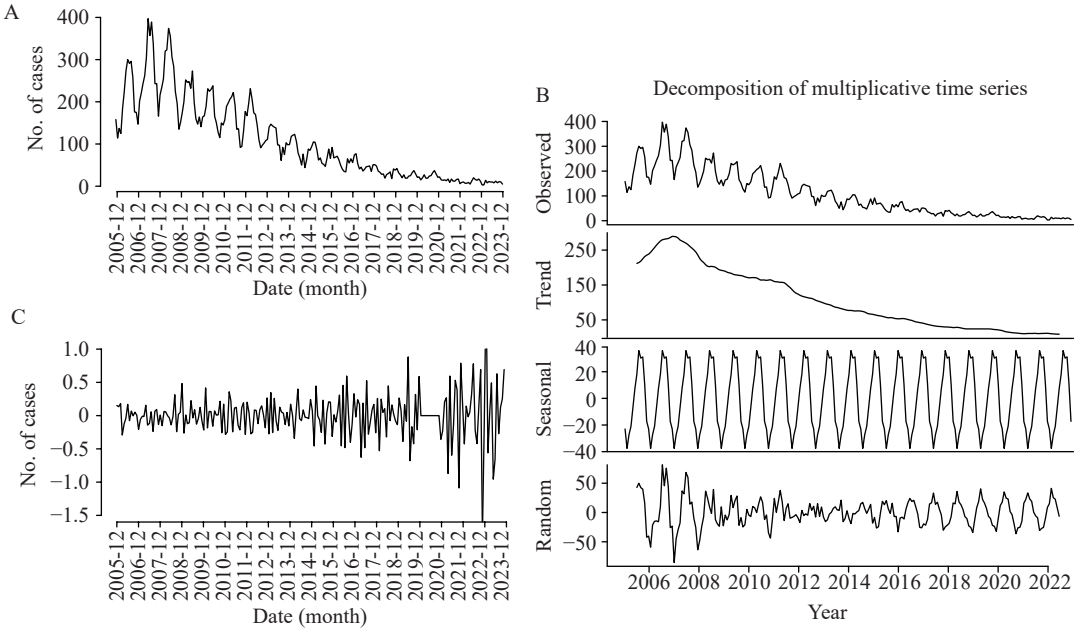

FIGURE 2. Time series of monthly incidence data of human rabies in China from 2005 to 2023. (A) Sequence diagram of the original sequence; (B) Trend, seasonal, and residual components derived from seasonal-trend decomposition of monthly incidence of human rabies; (C) Sequence diagram after natural logarithm transformation and first-step differencing and seasonal differencing with a period of 12 months.

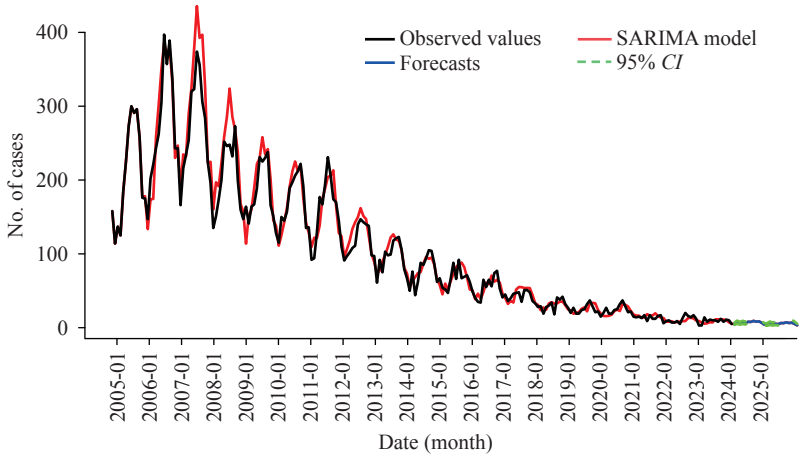

FIGURE 3. SARIMA $(0,1,2)(2,1,1)_{12}$ model fitting, validation, and prediction based on monthly human rabies incidence data in China from January 2005 to December 2023.
Note: The black line represents the actual value, the red line represents the fitting value, and the green line represents the 95% *CI*.
Abbreviation: *CI*=confidence interval.

TABLE 2. Comparison of rabies elimination progress among different countries.

Country	Pre-elimination cases			Elimination year
	15 years	10 years	5 years	
USA	2	3	2	2007
Japan	–	<10	<10	1956
Brazil	23	5	2	2016
China	801	202	65	2030

Note: "–" represents missing data.

Except for an increase from 2005 to 2007, the number of rabies cases has steadily decreased to 120 in 2023, representing a 96.36% reduction from the peak of 3,300 cases in 2007. The number of affected regions reached its lowest point in 2022, a 42.86% reduction from the peak observed in 2013. Annual cases along the southwest and southeast borders have significantly decreased. The proportion of cases in Guizhou dropped from 19.55% in 2006 to 1.67% in 2023, exemplifying effective control in traditional high-incidence areas. Recent policies, including the "National Medium and Long-term Animal Epidemic Prevention Planning (2012–2020)," "National Animal Rabies Prevention and Control Plan (2017–2020)," and "Law of the People's Republic of China on Animal Epidemic Prevention," have enhanced animal management and immunization, especially for dogs (*7*). The updated "Interpretation of the National Regulation for the Rabies Exposure Prophylaxis (2023 Edition)" further refined post-exposure procedures to achieve standardization and consistency. These ongoing efforts reflect continued improvement in rabies control across the country.

The prevalence of rabies, a natural zoonotic disease primarily spread by domestic dogs, has declined in China, but previously rabies-free areas remain vulnerable to reintroduction. For example, regions in northeast and western China with historically few outbreaks experienced re-emergence in Liaoning and Ningxia after being rabies-free for six years (2005–2010) and eight years (2003–2010), respectively (*12*). Virus traceability and spatial clustering analyses indicated that the outbreak in Ningxia resulted from pathogens spreading from Inner Mongolia (*13*). The Qinghai–Xizang Plateau, isolated and sparsely populated, remained rabies-free for over a decade but began reporting cases in Qinghai and Xizang in 2012 and 2015, respectively. With cases emerging in Xizang, rabies has now been reported in all PLADs (*12*). Animal hosts can bypass both natural barriers and national borders. In 2017, cases in Shigatse and Nagqu of Xizang were traced to Nepalese strains crossing the border (*14*). These examples highlight that without an immune barrier in host animal populations, eliminating rabies remains unattainable.

As shown in Table 2, rabies cases in China are expected to reach 65 by 2025, which is higher than the case numbers in Japan, the USA, and Brazil, 15 years before their respective elimination dates. Thus, China faces the challenge of achieving in five years what took other countries over 15 years to accomplish. Despite differences in economic development and policy

implementation, the successful elimination of rabies in these countries provides valuable lessons for understanding the challenges and urgency of rabies elimination in China. Dog vaccination is a proven and cost-effective strategy (*15*). Drawing from global experiences, the following measures should be adopted for dog management and vaccination efforts in China: 1) establish an authoritative body to coordinate departmental efforts; 2) ensure clear departmental responsibilities, focusing on comprehensive coverage for rural and stray dogs; and 3) conduct phased evaluations of program effectiveness, while continually monitoring dog infection and vaccination rates. Notably, strong policies and decisive implementation are central guarantees for effective prevention and control.

Rabies is a serious infectious disease that threatens public health. After 20 years of prevention and control efforts, rabies transmission in China has shifted from widespread to localized, indicating progress towards elimination. However, rabies will not disappear without concerted action. Strong policies and effective implementation are crucial to establishing robust dog vaccination defenses. Given time constraints and the complexity of the task, the One Health concept must be embraced to eliminate dog-to-human rabies by 2030.

Conflicts of interest: No conflicts of interest.

Acknowledgements: The authors gratefully acknowledge the assistance provided by all members of the Department of Rabies, National Institute for Viral Disease Control and Prevention, Chinese Center for Disease Control and Prevention.

Ethical statement: The National Health Commission of the People's Republic of China determined that rabies case collection is integral to public health surveillance and is exempted from institutional review board approval.

doi: 10.46234/ccdcw2025.163

[#] Corresponding authors: Xiaoyan Tao, taoxy@ivdc.chinacdc.cn; Wuyang Zhu, zhuwy@ivdc.chinacdc.cn.

[1] National Key Laboratory of Medical Viruses and Viral Diseases, National Institute for Viral Disease Control and Prevention, Chinese Center for Disease Control and Prevention, Beijing, China.

Submitted: August 26, 2024
Accepted: April 08, 2025
Issued: July 18, 2025

REFERENCES

1. Badrane H, Tordo N. Host switching in *Lyssavirus* history from the chiroptera to the carnivora orders. J Virol 2001;75(17):8096 – 104. https://doi.org/10.1128/jvi.75.17.8096-8104.2001.
2. Ruan SG. Modeling the transmission dynamics and control of rabies in China. Math Biosci 2017;286:65 – 93. https://doi.org/10.1016/j.mbs.2017.02.005.
3. Hampson K, Coudeville L, Lembo T, Sambo M, Kieffer A, Attlan M, et al. Estimating the global burden of endemic canine rabies. PLoS Negl Trop Dis 2015;9(4):e0003709. https://doi.org/10.1371/journal.pntd.0003709.
4. The Lancet. Time to eliminate rabies. Lancet 2015;386(10012):2446. https://doi.org/10.1016/S0140-6736(15)01287-8.
5. World Health Organization. WHO expert consultation on rabies. Geneva: WHO; 2018. https://iris.who.int/handle/10665/272364.
6. Lv MM, Sun XD, Jin Z, Wu HR, Li MT, Sun GQ, et al. Dynamic analysis of rabies transmission and elimination in mainland China. One Health 2023;17:100615. https://doi.org/10.1016/j.onehlt.2023.100615.
7. Shen TR, Welburn SC, Sun L, Yang GJ. Progress towards dog-mediated rabies elimination in PR China: a scoping review. Infect Dis Poverty 2023;12(1):30. https://doi.org/10.1186/s40249-023-01082-3.
8. Tao XY, Liu SQ, Zhu WY, Rayner S. Rabies surveillance and control in China over the last twenty years. Biosaf Health 2021;3(3):142 – 7. https://doi.org/10.1016/j.bsheal.2020.11.004.
9. Pieracci EG, Pearson CM, Wallace RM, Blanton JD, Whitehouse ER, Ma XY, et al. *Vital signs*: trends in human rabies deaths and exposures - United States, 1938-2018. MMWR Morb Mortal Wkly Rep 2019;68(23):524 – 8. https://doi.org/10.15585/mmwr.mm6823e1.
10. Kanda K, Jayasinghe A, Jayasinghe C, Yoshida T. Maintenance of rabies-free status in Japan for 65 years and application of lessons learned to other countries working towards zero human deaths. In: Slack V, Nadal D, Yasobant S, Cliquet F, Ahmad W, Pushpakumara N, et al, editors. One health for dog-mediated rabies elimination in Asia: a collection of local experiences. Boston: CABI. 2023; p. 235-47. http://dx.doi.org/10.1079/9781800622975.0019.
11. Schneider MC, Min KD, Romijn PC, De Morais NB, Montebello L, Rocha SM, et al. Fifty years of the national rabies control program in Brazil under the one health perspective. Pathogens 2023;12(11):1342. https://doi.org/10.3390/pathogens12111342.
12. Tao XY, Guo ZY, Li H, Jiao WT, Shen XX, Zhu WY, et al. Rabies cases in the west of China have two distinct origins. PLoS Negl Trop Dis 2015;9(10):e0004140. https://doi.org/10.1371/journal.pntd.0004140.
13. Tao XY, Li ML, Guo ZY, Yan JH, Zhu WY. Inner Mongolia: a potential portal for the spread of rabies to Western China. Vector Borne Zoonotic Dis 2019;19(1):51 – 8. https://doi.org/10.1089/vbz.2017.2248.
14. Tao XY, Li ML, Wang Q, Baima C, Hong M, Li W, et al. The reemergence of human rabies and emergence of an Indian subcontinent lineage in Tibet, China. PLoS Negl Trop Dis 2019;13(1):e0007036. https://doi.org/10.1371/journal.pntd.0007036.
15. Wang DL, Zhang XF, Wang XC, Wang YT, Zhang R, Chen YY, et al. Cost-effectiveness analysis of rabies immunization strategy based on dynamic-decision tree model. Chin J Prev Med 2019;53(8):804 – 10. https://doi.org/10.3760/Cma.J.Issn.0253-9624.2019.08.002.

SUPPLEMENTARY MATERIAL

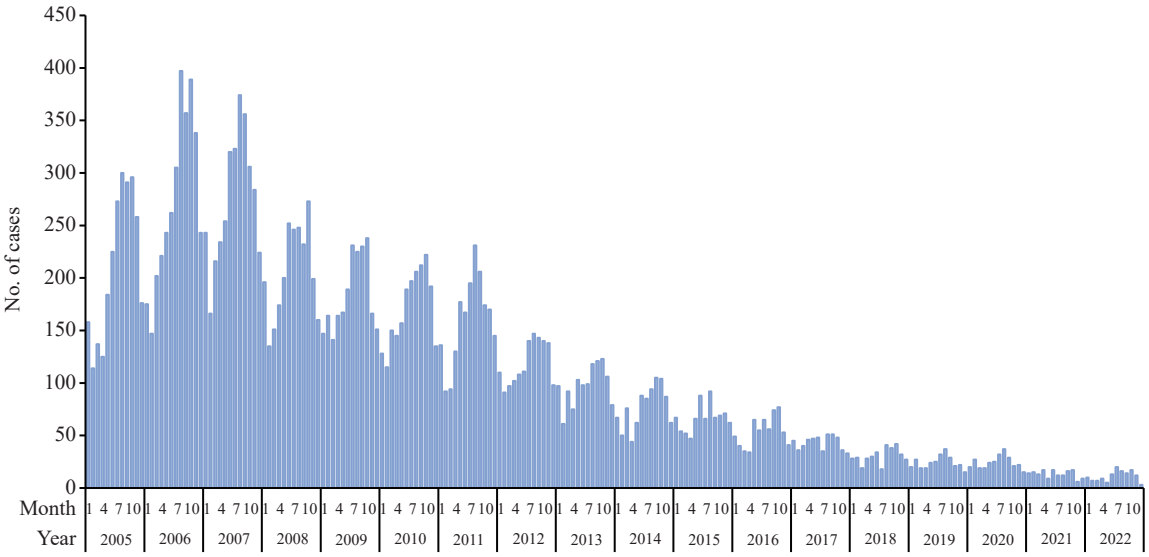

SUPPLEMENTARY FIGURE S1. Monthly distribution of human rabies cases in China from 2005 to 2022.

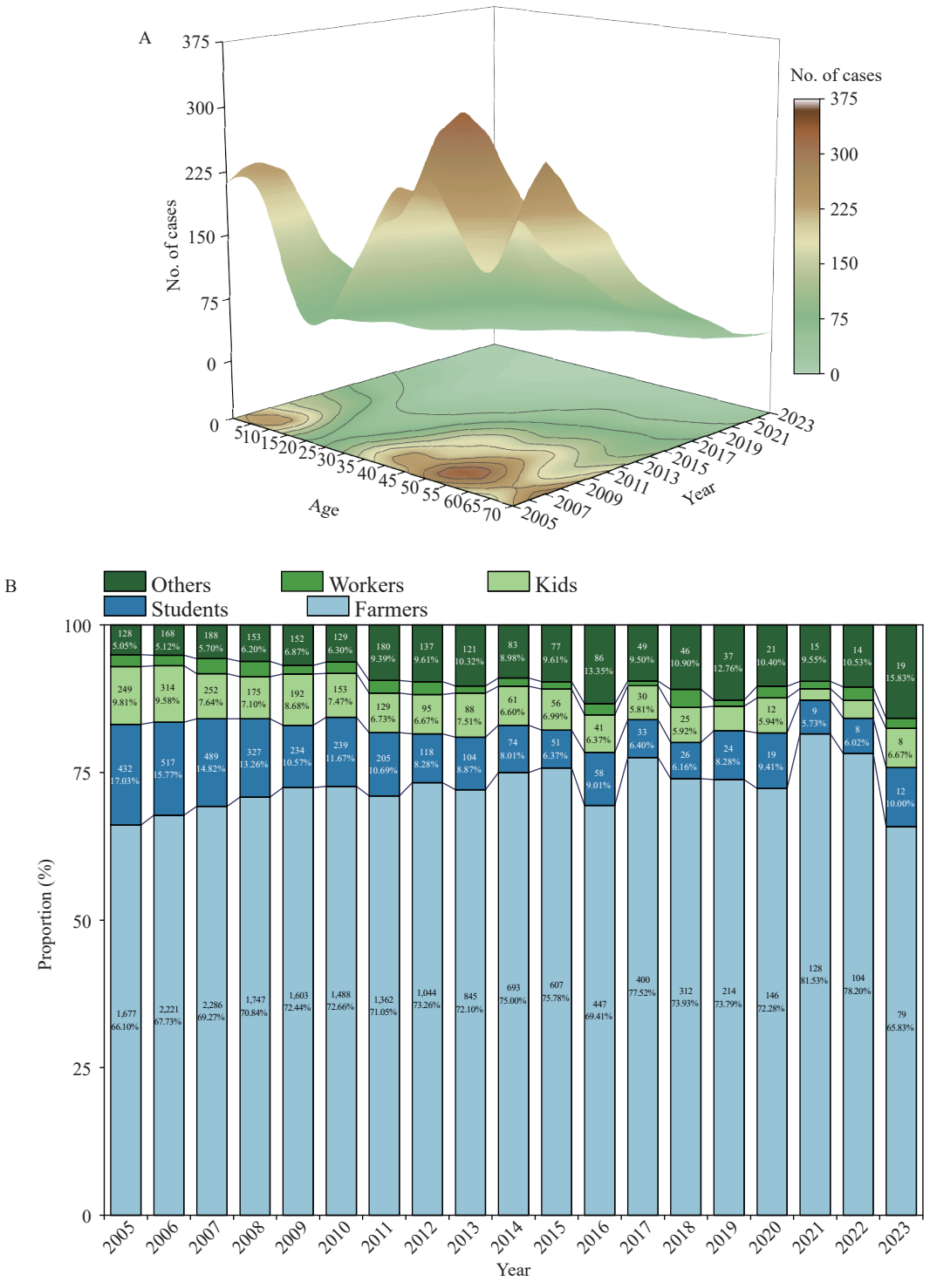

SUPPLEMENTARY FIGURE S2. Demographic characteristics of human rabies cases in China, 2005–2022. The distribution of human rabies cases by (A) age and (B) occupation.

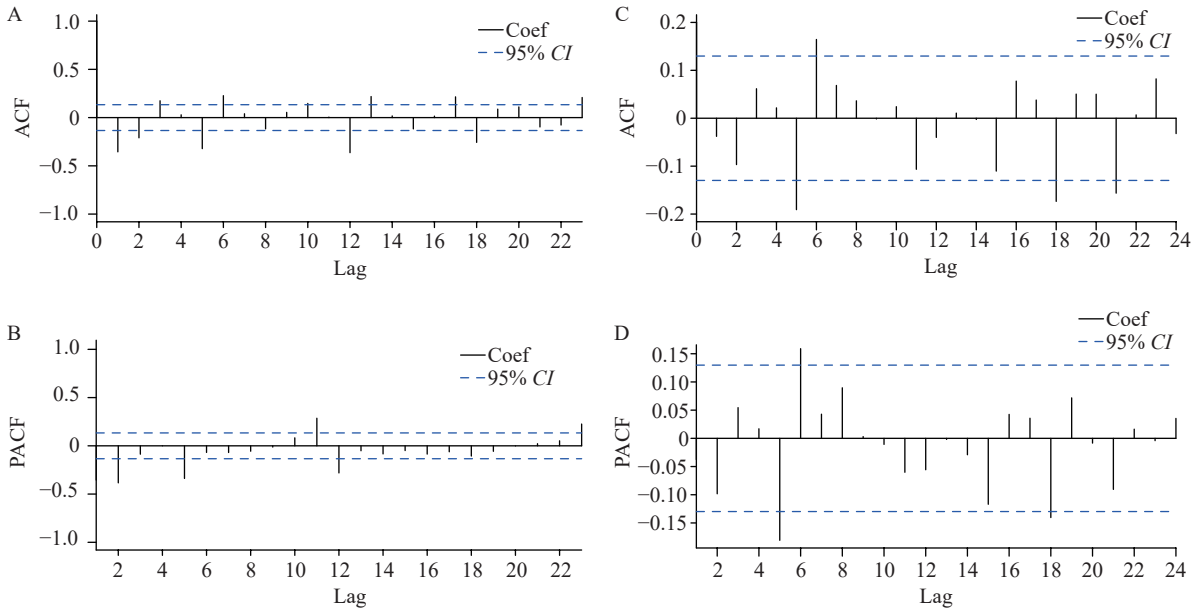

SUPPLEMENTARY FIGURE S3. Autocorrelation function (ACF) and partial autocorrelation function (PACF) plots of the differencing human rabies cases. (A) ACF plot of the seasonal differential series. (B) PACF plot of the seasonal differential series. (C) ACF plot of residuals after applying the SARIMA $(0,1,2)(2,1,1)_{12}$ model. (D) PACF plot of residuals after applying the SARIMA $(0,1,2)\ (2,1,1)_{12}$ model.
Note: The number of lags is plotted along the *x* axis and the correlation coefficient (−1 to 1) along the *y* axis. Dotted lines indicate 95% *CI*.
Abbreviation: *CI*=confidence interval.

SUPPLEMENTARY TABLE S1. Fitting parameters of eight possible SARIMA models.

Models	AIC	BIC	Log-likelihood	Weighted average
SARIMA $(0,1,2)\ (2,1,1)_{12}$	−7.1	13.12	9.55	−4.36
SARIMA $(0,1,2)\ (0,1,1)_{12}$	−6.08	7.4	7.04	−4.26
SARIMA $(2,1,1)\ (2,1,1)_{12}$	−7.14	16.45	10.6	−3.94
SARIMA $(2,1,1)\ (0,1,1)_{12}$	−5.94	10.91	7.97	−3.66
SARIMA $(1,1,1)\ (0,1,1)_{12}$	−5.16	8.32	6.58	−3.33
SARIMA $(1,1,2)\ (2,1,1)_{12}$	−6.45	17.14	10.23	−3.25
SARIMA $(0,1,1)\ (0,1,1)_{12}$	−4.62	5.49	5.31	−3.25
SARIMA $(1,1,2)\ (0,1,1)_{12}$	−5.33	11.52	7.67	−3.05

Abbreviation: AIC=Akaike Information Criterion; BIC= Bayesian Information Criterion; SARIMA=Seasonal autoregressive integrated moving average.

SUPPLEMENTARY TABLE S2. Parameter estimation and verification of the SARIMA $(0,1,2)\ (2,1,1)_{12}$ model.

Variables	Estimates	Standard Error	t	*P*
MA 2	−0.191	0.071	2.681	0.008
SAR 2	−0.277	0.125	−2.213	0.028
SMAR 1	0.525	0.151	3.474	0.001

Abbreviation: SARIMA=seasonal autoregressive integrated moving average; MA=moving average; SAR=seasonal autoregressive; SMAR=seasonal moving average regressive; *CI*=confidence Interval.

SUPPLEMENTARY TABLE S3. Forecasts and 95% *CI*s of human rabies cases for the next 24 months based on the SARIMA $(0,1,2)(2,1,1)_{12}$ model.

Time	Forecasts	95% *CI*	Time	Forecasts	95% *CI*
24-January	5.134	(3.167, 7.741)	25-January	4.043	(2.216, 7.072)
24-February	7.108	(4.561, 11.819)	25-February	5.598	(2.665, 8.729)
24-March	5.670	(3.444, 9.067)	25-March	4.465	(2.159, 7.205)
24-April	6.766	(4.199, 11.229)	25-April	5.328	(2.664, 9.058)
24-May	6.004	(3.302, 8.964)	25-May	4.728	(1.901, 6.582)
24-June	8.036	(4.614, 12.716)	25-June	6.328	(3.125, 11.018)
24-July	7.825	(4.210, 11.773)	25-July	6.162	(3.272, 11.743)
24-August	9.215	(4.808, 13.645)	25-August	7.257	(3.389, 12.375)
24-September	8.094	(4.443, 12.791)	25-September	6.374	(3.064, 11.385)
24-October	8.639	(4.582, 13.379)	25-October	6.804	(3.303, 12.481)
24-November	6.553	(2.994, 8.864)	25-November	5.160	(2.204, 8.469)
24-December	4.033	(2.219, 6.662)	25-December	3.175	(1.205, 4.709)
Total	83.077	(46.543, 128.650)	Total	65.422	(31.167, 110.826)

Abbreviation: SARIMA=seasonal autoregressive integrated moving average; *CI*=confidence Interval.

Methods and Applications

Mapping the Global Antigenic Evolution of Human Influenza A/H3N2 Neuraminidase Based on a Machine Learning Model — 1968–2024

Jingru Feng[1,&]; Rui Shi[2,&]; Huixin Zhou[3,&]; Shijie Wu[1,2]; Junyu Hu[1,2]; Taijiao Jiang[4,5,6]; Wenjie Han[2,#]; Xiangjun Du[1,3,7,#]

ABSTRACT

Introduction: Human influenza A/H3N2 imposes a substantial global disease burden. Beyond hemagglutinin (HA), neuraminidase (NA) also plays a critical role in the antigenic evolution of influenza viruses. However, a comprehensive understanding of NA antigenic evolution remains lacking.

Methods: NA inhibition (NAI) data were collected and structural epitopes for A/H3N2 NA were identified. A machine learning model was developed to accurately predict antigenic relationships by integrating four feature groups: epitopes, physicochemical properties, N-glycosylation, and catalytic sites. An antigenic correlation network (ACNet) was constructed and antigenic clusters were identified using the Markov clustering algorithm.

Results: The best random forest model (PREDEC-N2) achieved an accuracy of 0.904 in cross-validation and 0.867 in independent testing. Eight main antigenic clusters were identified on the ACNet. Spatiotemporal analysis revealed the continuous replacement and rapid global spread of new antigenic clusters for human influenza A/H3N2 NA.

Conclusions: This study developed a timely and accurate computational model to map the antigenic landscape of A/H3N2 NA, revealing both its relative antigenic conservation and continuous evolution. These insights provide valuable guidance for improved antigenic surveillance, vaccine recommendations, and prevention and control strategies for human influenza viruses.

Human influenza A/H3N2 has been a predominant seasonal influenza strain globally since its emergence in 1968. The main surface proteins of the influenza virus, hemagglutinin (HA) and neuraminidase (NA), evolve antigenically to escape immune recognition by the human host (*1*). Vaccination is the most effective intervention against influenza, but the vaccine effectiveness (VE) against H3N2 remains low (*2*). This low VE is mainly attributable to the rapid antigenic drift of HA and the insufficient induction of a robust NA-mediated immune response by current vaccines (*2*). Several studies have highlighted the critical role of NA-induced protection (*3*). Compared to human influenza A/H1N1, the antigenic divergence of NA in A/H3N2 is minimal but antigenic changes still occur (*4*). However, the antigenic evolution and landscape of NA in human influenza A/H3N2 remain poorly understood. To address this gap, we developed an antigenic classification model for human influenza A/H3N2 NA and identified distinct antigenic clusters to provide a more systematic understanding of the antigenic evolution of NA.

METHODS

Sequence Data

NA sequences of human influenza A/H3N2 viruses, available up to October 2024, were downloaded from global initiative on sharing all influenza data (GISAID) (*5*). To mitigate sampling bias, we implemented an even sampling strategy. Seven representative sequences were randomly selected for each month and each continent; if fewer than seven sequences were available, all sequences were included. Sequences containing more than three ambiguous amino acids or fewer than 400 residues in length were excluded. Subsequently, multiple sequence alignment was conducted, and three sequences with insertion mutations present in fewer than 1% of the sampled sequences were removed. The alignment was then repeated, resulting in a final sequence length of 469 amino acid residues. Sequence alignment and phylogenetic tree construction were performed using methods described in previous studies

(*6*). Finally, 9,054 sequences were analyzed.

A proportional sampling strategy was also implemented to avoid sampling error, selecting 5% of the sequences per month from each continent, or one sequence if the calculated sample size was less than one. After quality control, 7,847 sequences were retained for analysis.

NAI Data

A total of 376 pairs of NA inhibition (NAI) data were collected from various sources (*4*,*7*–*10*). For strain pairs tested in multiple experiments, the median result was used as the final value. The antigenic distance between two strains was calculated using the following formula (*11*):

$$H_{ab} = \sqrt{\frac{T_{aa}T_{bb}}{T_{ab}T_{ba}}} \quad (1)$$

where H_{ab} represents the NA antigenic distance between strain a and strain b, T_{ab} and T_{bb} are the NAI titers of serum b against virulent strains a and b, and T_{aa} and T_{ba} are the NAI titers of serum a against virulent strains a and b. A pair of strains was classified as antigenically similar if the absolute value of their antigenic distance was between 0.25 and 4 (not equal); otherwise, the pair was considered antigenically dissimilar.

Feature Selection

Twelve features were used to construct machine learning (ML) models based on NA sequences, which were categorized into four groups: epitopes, physicochemical properties, N-glycosylation, and catalytic sites.

Epitopes We used 7U4E as a template to identify potential structural epitopes. Sites with a binding probability above 0.1, as determined by ScanNet (*12*), were identified as potential epitope sites. K-means clustering was performed using spatial coordinates to determine the number of epitopes and composition of each epitope based on the Silhouette score (Supplementary Figure S1, available at https://weekly.chinacdc.cn/). Outliers that were excessively distant from other clusters were excluded, resulting in the identification of five epitopes (N2_A, N2_B, N2_C, N2_D, and N2_E, Supplementary Figure S2 and Supplementary Table S1, available at https://weekly.chinacdc.cn/). For each epitope, features were quantified by calculating the number of amino acid changes.

Physicochemical Properties Five classes of physicochemical properties were considered: hydrophobicity, charge, polarity, volume, and accessible surface area (ASA). A random forest (RF) model was trained on the training dataset to identify the best representative feature for each class. The selected indices were CHAM830107, RADA880108, CIDH920101, CHOC760102, and COHE430101. Features were computed by averaging the absolute differences between sequence pairs based on up to the three most prominent changes.

N-Glycosylation sites (N-Glycosylation) N-Glycosylation sites were identified using NetNGlyc (*13*), and the numbers of different glycosylation sites were calculated.

Catalytic sites (Catalyze) Eight previously reported NA catalytic sites were included, and the average Euclidean distances to the catalytic sites were calculated for each amino acid position, from which the three shortest distances were selected (*14*).

Model Construction

The antigenically similar or dissimilar label were used to train the model based on the 12-bit features calculated above. Five ML models capable of handling non-linear data were constructed using the Python package scikit-learn and evaluated: logistic regression (LR), support vector machine (SVM), K-nearest neighbors (KNN), RF, and extreme gradient boosting (XGBoost). We randomly split 70% of the NAI pairs for the training set and reserved the remaining 30% for the testing set. Model parameters were optimized using 5-fold cross-validation combined with random search conducted 500 times on the training set. The models were evaluated using five metrics: accuracy, precision, F1-score, recall, and receiver operating characteristic area under the curve (ROC-AUC).

Construction of Antigenic Network

The antigenic correlation network (ACNet) was constructed and visualized using Cytoscape (version 3.10.2, developed by Cytoscape Consortium, San Diego, United States). In this network, nodes represent NA strains and edges indicate antigenic similarity relationships as predicted by the model. The Markov cluster algorithm was used to identify clusters of strains based on the logarithmic ratio of the probabilities of antigenic similarity to dissimilarity. Clustering parameters were selected by optimizing mean cluster sizes and modularity (Supplementary Figure S3, available at https://weekly.chinacdc.cn/).

RESULTS

Antigenic Prediction Model for NA of Human Influenza A/H3N2

Five ML models were constructed using cross-validation (Supplementary Figure S4, available at https://weekly.chinacdc.cn/) and evaluated using the testing set (Figure 1A). The RF model outperformed all other models across all metrics, achieving the highest ROC-AUC value of 0.849 and the highest accuracy of 0.867 on the test set. Therefore, the RF model was selected for subsequent analyses. Analysis of feature contributions revealed varying importance among different features (Figure 1B and C). Physicochemical properties contributed the most (39.1%), followed by epitopes (32.7%), catalytic sites (21.7%), and N-glycosylation sites (6.5%). The catalytic sites feature had the greatest individual impact, contributing approximately 21.7%. Among epitope-related features, Epitopes N2_D, N2_B, and N2_C, which are located near catalytic sites (Supplementary Figure S2), were identified as the most significant, indicating their critical role in both viral

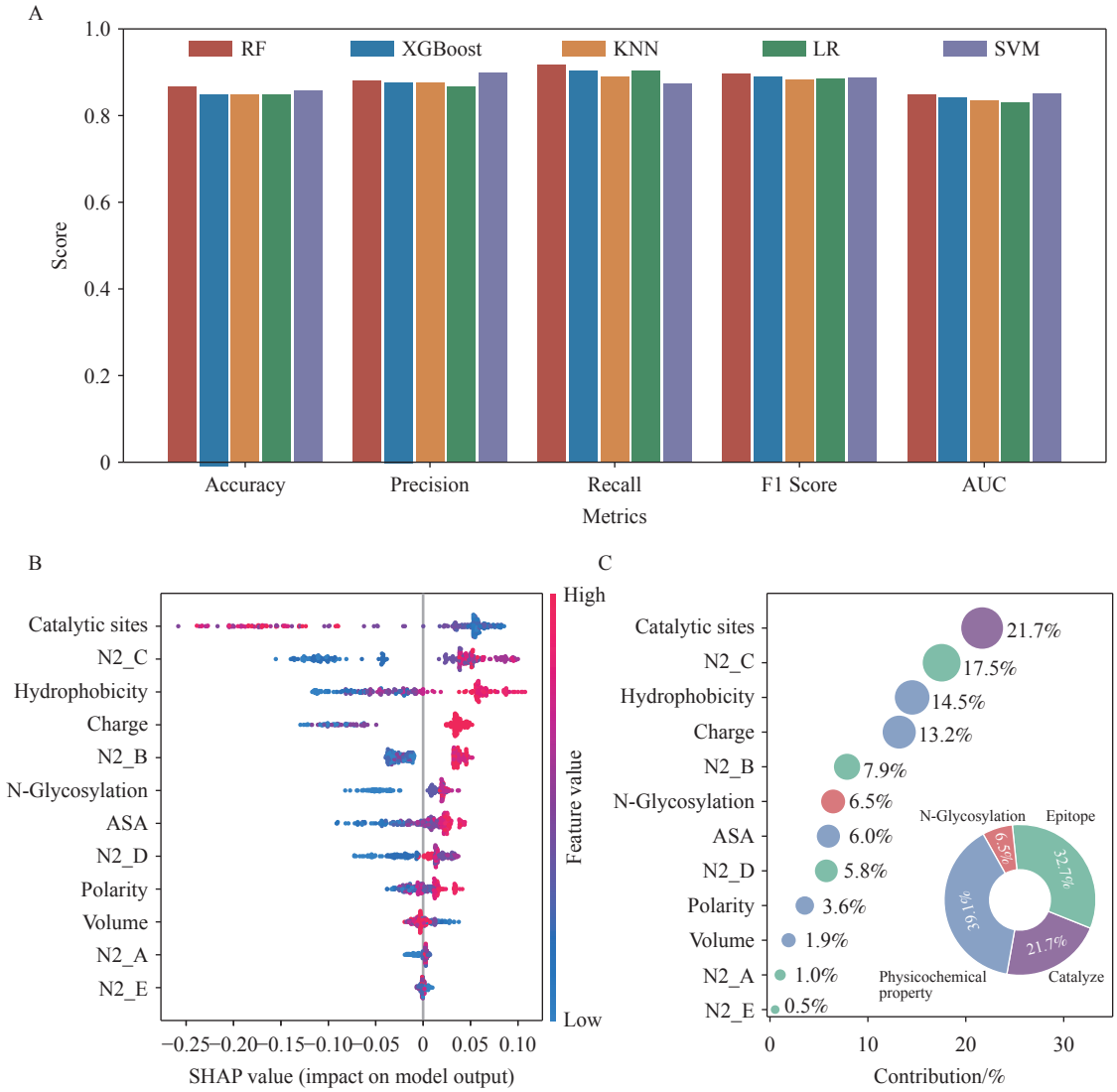

FIGURE 1. Model performance and feature contributions. (A) Model performance on the independent testing set; (B) Feature contributions at the sample level, where color indicates the magnitude and position reflects the absolute contribution of each feature; (C) Feature contributions at the population level.

Note: Different groups were color-coded, and size represents the magnitude of individual features. Abbreviation: RF=random forest; XGBoost=extreme gradient boosting; KNN=K-nearest neighbors; LR=logistic regression; SVM=support vector machine; AUC=receiver operating characteristic area under the curve; ASA=access surface area; SHAP=SHapley Additive exPlanation.

function and prediction (Figure 1C). The epitope located at the junction of different chains (N2_A) was less important, contributing only 1% to the overall feature importance.

The Antigenic Landscape for NA of Human Influenza A/H3N2

Based on the RF model, we predicted antigenic relationships between all representative strains for NA of human influenza A/H3N2 and constructed an ACNet for evenly sampled sequences. We identified eight major antigenic clusters that aligned with the traditional phylogenetic tree (Figure 2A). These clusters, which included vaccine strains, were named after the earliest vaccine strain within each cluster: PC73, TE77, BJ89, WH95, MS99, CA04, PE09, and SI16 (Supplementary Table S2, available at https://weekly.chinacdc.cn/). We validated the clustering by demonstrating that strains within the same cluster were more antigenically similar than those from different clusters (Supplementary Figure S5, available at https://weekly.chinacdc.cn/). A clear spatiotemporal pattern emerged: new clusters appeared and gradually replaced older ones, a trend observed consistently across different continents (Figure 2B and Supplementary Figure S6, available at https://weekly.chinacdc.cn/). Furthermore, NA antigenic clusters exhibited greater persistence over time (approximately 8 years) compared with HA (approximately 2 or 3 years) (Figure 2C) (*15*). The clustering and prevalence analyses from proportional sampling were largely consistent with these findings (Supplementary Figure S7, available at https://weekly.chinacdc.cn/).

DISCUSSION

In the present study, we developed a novel machine learning model for timely and effective prediction of antigenic relationships in the neuraminidase of human influenza A/H3N2. We identified eight main antigenic clusters between 1968 and 2024. Spatiotemporal analysis revealed continuous global replacement and rapid spread of new antigenic clusters. Our findings were robust across different sampling approaches. Among forty-eight vaccine strains, only one (A/Wellington/01/2004) during the cluster transition period was classified differently, likely due to significant differences in sequence distribution.

The antigenic prediction model for NA was developed using an approach similar to that for HA. A key adjustment was replacing the receptor-binding features of HA with catalytic sites, which are more pertinent to NA function. Additionally, we identified NA epitopes de novo for feature calculation. While these adjustments did not represent significant innovations, the framework has proven effective with only minor modifications across different contexts (*16*). This suggests that with appropriate adjustments, our model can provide accurate predictions for NA antigenic correlations.

Both antigenic clusters and phylogenetic clades reflect evolutionary relationships between viral strains, representing phenotype and genotype, respectively. Unlike the continuous branching of phylogeny, antigenic clusters represent important discrete phenotypes for HA and NA, with nonlinear relationships to genetic changes (*4*). Variations at different sites have inconsistent effects on antigenicity. The phylogenetic tree for NA displayed a single-trunk structure, indicating minimal selection pressure. Furthermore, spatiotemporal analysis confirmed the continuous global replacement of older antigenic clusters by newer ones. Only eight major antigenic clusters were identified for NA over the past 60 years (approximately one cluster every 8 years), significantly fewer than for HA (approximately every 2 or 3 years). This phenomenon might be explained by the relatively lower mean rate of nucleotide substitution in NA, which could be partly attributed to stronger structural constraints on this enzyme compared to the receptor-binding protein, as well as the stronger selection pressure and greater immune pressure on HA, likely due to its role as the primary vaccine target and its higher distribution on the virus surface (*17–18*).

This study has several limitations that warrant consideration. First, while our dataset was sufficient for model development, a larger dataset would enable the construction of more sophisticated models with improved prediction performance. Second, although we developed the first ML antigenic classification model for NA, integration with HA and other important viral components is necessary for a comprehensive understanding of antigenic evolution and its implications for seasonal influenza. Third, due to variations in sequencing coverage, some regions had insufficient sequence data, leading to incomplete characterization of their antigenic landscapes. Similarly, the analysis of early antigenic clusters may be subject to sequencing bias. Finally, while our model demonstrated high predictive accuracy, validation with experimental data or real-world outcomes would further strengthen its applicability.

The findings of this study highlight the crucial role of NA in the antigenic evolution of human influenza A/H3N2 and its contribution to viral circulation and

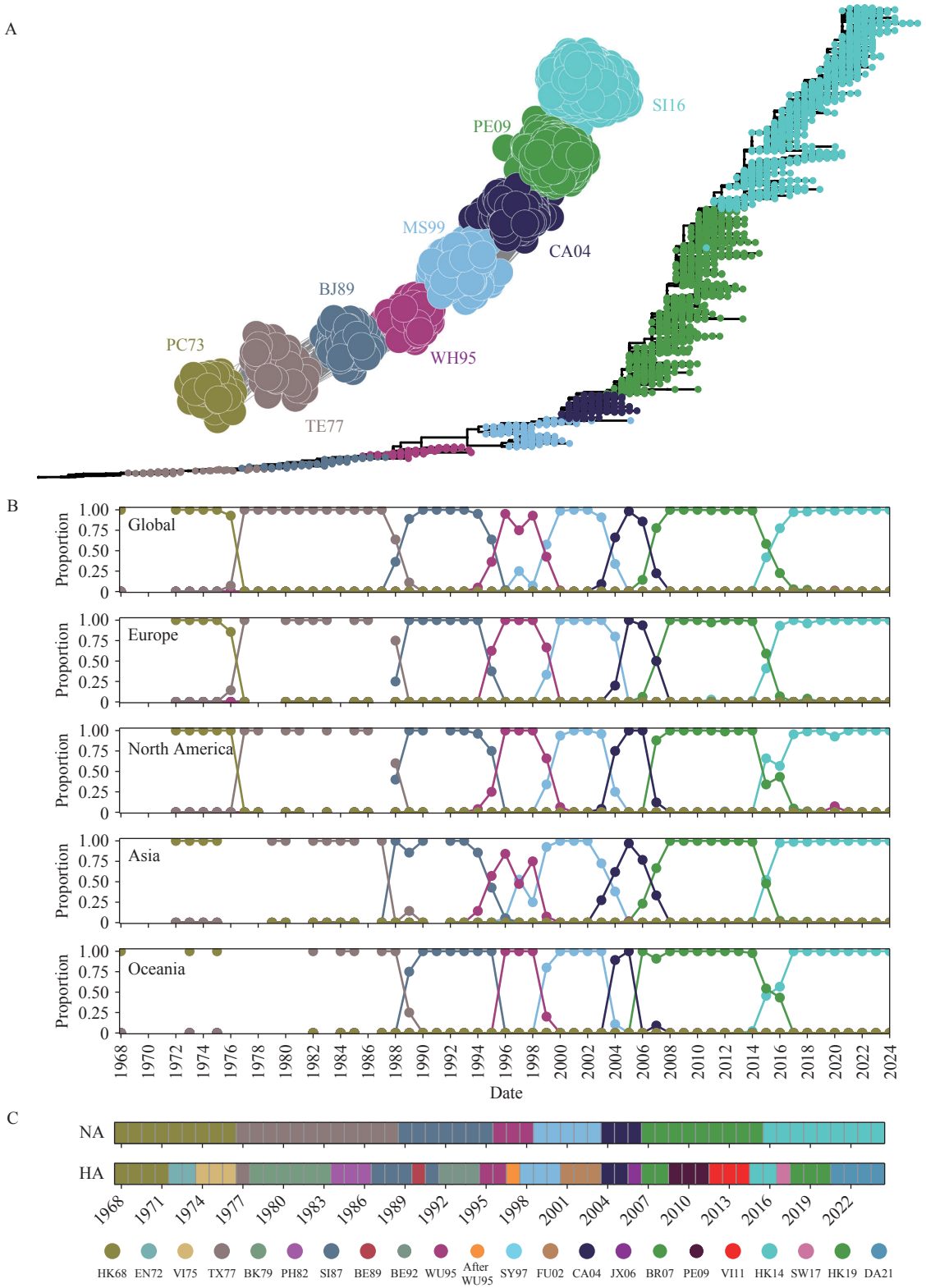

FIGURE 2. Antigenic landscape of A/H3N2 NA. (A) The ACNet and phylogenetic tree for representative sequences from eight major antigenic clusters; (B) Yearly spatiotemporal distribution of eight antigenic clusters; (C) Replacement patterns of dominant antigenic clusters.
Note: The legend displays colors for HA while the color of NA antigenic clusters correspond to those used in the ACNet. For (C), color changes indicating that a new antigenic cluster is dominant or becoming dominant.
Abbreviation: NA=neuraminidase; HA=hemagglutinin; ACNet=antigenic correlation network.

spread. Although NA currently receives less consideration in vaccine strain recommendation and antigenic surveillance, the tools developed in this study can facilitate improved antigenic monitoring, inform vaccine selection, and ultimately aid in the prevention and control of influenza epidemics as knowledge deepens and relevant technologies advance.

Conflicts of interest: No conflicts of interest.

Acknowledgements: We gratefully acknowledge all the authors from the original laboratories who submitted and shared data on which this study is based. This work was supported by the BrightWing High-performance Computing Platform, School of Public Health (Shenzhen), and High-performance Computing Public Platform (Shenzhen Campus), Sun Yat-sen University.

Funding: Supported by the National Key Research and Development Program under grant 2022YFC2303800, the Major Program of Guangzhou National Laboratory under grant GZNL2024A01002, the National Natural Science Foundation of China under grant 81961128002, the Science and Technology Planning Project of Guangdong Province, China under grant 2021B1212040017, and the Shenzhen Science and Technology Program under grant ZDSYS20230626091203007.

doi: 10.46234/ccdcw2025.164

[#] Corresponding authors: Wenjie Han, hanwj7@mail2.sysu.edu.cn; Xiangjun Du, duxj9@mail.sysu.edu.cn.

[1] School of Public Health (Shenzhen), Sun Yat-sen University, Guangzhou City, Guangdong Province, China; [2] School of Public Health (Shenzhen), Shenzhen Campus of Sun Yat-sen University, Shenzhen City, Guangdong Province, China; [3] Shenzhen Key Laboratory of Pathogenic Microbes & Biosafety, Shenzhen Campus of Sun Yat-sen University, Shenzhen City, Guangdong Province, China; [4] Guangzhou National Laboratory, Guangzhou City, Guangdong Province, China; [5] State Key Laboratory of Respiratory Disease, The Key Laboratory of Advanced Interdisciplinary Studies Center, the First Affiliated Hospital of Guangzhou Medical University, Guangzhou City, Guangdong Province, China; [6] Suzhou Institute of Systems Medicine, Suzhou City, Jiangsu Province, China; [7] Key Laboratory of Tropical Disease Control, Ministry of Education, Sun Yat-sen University, Guangzhou City, Guangdong Province, China.
[&] Joint first authors.

Submitted: October 22, 2024
Accepted: May 28, 2025
Issued: July 18, 2025

REFERENCES

1. Petrova VN, Russell CA. The evolution of seasonal influenza viruses. Nat Rev Microbiol 2018;16(1):47 – 60. https://doi.org/10.1038/nrmicro.2017.118.
2. Chen YQ, Wohlbold TJ, Zheng NY, Huang M, Huang YP, Neu KE, et al. Influenza infection in humans induces broadly cross-reactive and protective neuraminidase-reactive antibodies. Cell 2018;173(2):417 – 29.e10. https://doi.org/10.1016/j.cell.2018.03.030.
3. Weiss CD, Wang W, Lu Y, Billings M, Eick-Cost A, Couzens L, et al. Neutralizing and neuraminidase antibodies correlate with protection against influenza during a late season A/H3N2 outbreak among unvaccinated military recruits. Clin Infect Dis 2020;71(12):3096 – 102. https://doi.org/10.1093/cid/ciz1198.
4. Sandbulte MR, Westgeest KB, Gao J, Xu XY, Klimov AI, Russell CA, et al. Discordant antigenic drift of neuraminidase and hemagglutinin in H1N1 and H3N2 influenza viruses. Proc Natl Acad Sci USA 2011;108 (51):20748 – 53. https://doi.org/10.1073/pnas.1113801108.
5. Khare S, Gurry C, Freitas L, Schultz MB, Bach G, Diallo A, et al. GISAID's role in pandemic response. China CDC Wkly 2021;3(49): 1049 – 51. https://doi.org/10.46234/ccdcw2021.255.
6. Zhai K, Dong JZ, Zeng JF, Cheng PW, Wu XS, Han WJ, et al. Global antigenic landscape and vaccine recommendation strategy for low pathogenic avian influenza A (H9N2) viruses. J Infect 2024;89(2): 106199. https://doi.org/10.1016/j.jinf.2024.106199.
7. Catani JPP, Smet A, Ysenbaert T, Vuylsteke M, Bottu G, Mathys J, et al. The antigenic landscape of human influenza N2 neuraminidases from 2009 until 2017. eLife 2024;12:RP90782 https://doi.org/10.7554/eLife.90782.4.
8. Gao J, Li X, Klenow L, Malik T, Wan HQ, Ye ZP, et al. Antigenic comparison of the neuraminidases from recent influenza A vaccine viruses and 2019–2020 circulating strains. npj Vaccines 2022;7(1):79 https://doi.org/10.1038/s41541-022-00500-1.
9. Schild GC, Oxford JS, Dowdle WR, Coleman M, Pereira MS, Chakraverty P. Antigenic variation in current influenza A viruses: evidence for a high frequency of antigenic 'drift' for the Hong Kong virus. Bull World Health Organ 1974;51(1):1-11. https://pubmed.ncbi.nlm.nih.gov/4218138/.
10. Kilbourne ED, Johansson BE, Grajower B. Independent and disparate evolution in nature of influenza A virus hemagglutinin and neuraminidase glycoproteins. Proc Natl Acad Sci USA 1990;87(2): 786 – 90 https://doi.org/10.1073/pnas.87.2.786.
11. Meng J, Liu JZ, Song WK, Li HL, Wang JY, Zhang L, et al. PREDAC-CNN: predicting antigenic clusters of seasonal influenza A viruses with convolutional neural network. Brief Bioinform 2024;25(2):bbae033. https://doi.org/10.1093/bib/bbae033.
12. Tubiana J, Schneidman-Duhovny D, Wolfson HJ. ScanNet: an interpretable geometric deep learning model for structure-based protein binding site prediction. Nat Methods 2022;19(6):730 – 9. https://doi.org/10.1038/s41592-022-01490-7.
13. Blom N, Sicheritz-Pontén T, Gupta R, Gammeltoft S, Brunak S. Prediction of post-translational glycosylation and phosphorylation of proteins from the amino acid sequence. Proteomics 2004;4(6):1633 – 49. https://doi.org/10.1002/pmic.200300771.
14. Jagadesh A, Salam AAA, Mudgal PP, Arunkumar G. Influenza virus neuraminidase (NA): a target for antivirals and vaccines. Arch Virol 2016;161(8):2087 – 94. https://doi.org/10.1007/s00705-016-2907-7.
15. Du XJ, Dong LB, Lan Y, Peng YS, Wu AP, Zhang Y, et al. Mapping of H3N2 influenza antigenic evolution in China reveals a strategy for vaccine strain recommendation. Nat Commun 2012;3(1):709. https://doi.org/10.1038/ncomms1710.
16. Qiu JX, Qiu TY, Dong QL, Xu DP, Wang X, Zhang Q, et al. Predicting the antigenic relationship of foot-and-mouth disease virus for vaccine selection through a computational model. IEEE/ACM Trans Comput Biol Bioinf 2021;18(2):677 – 85. https://doi.org/10.1109/TCBB.2019.2923396.
17. Westgeest KB, de Graaf M, Fourment M, Bestebroer TM, van Beek R, Spronken MIJ, et al. Genetic evolution of the neuraminidase of influenza A (H3N2) viruses from 1968 to 2009 and its correspondence to haemagglutinin evolution. J Gen Virol 2012;93(9):1996 – 2007. https://doi.org/10.1099/vir.0.043059-0.
18. Harris A, Cardone G, Winkler DC, Heymann JB, Brecher M, White JM, et al. Influenza virus pleiomorphy characterized by cryoelectron tomography. Proc Natl Acad Sci USA 2006;103(50):19123 – 7. https://doi.org/10.1073/pnas.0607614103.

SUPPLEMENTARY MATERIAL

SUPPLEMENTARY TABLE 1. NA inhibition experimental data *(1–5)*.

The complete table is available at: https://zenodo.org/records/15653659 (uploaded on June 13, 2025).

SUPPLEMENTARY TABLE 2. Identified epitopes for human influenza A/H3N2 NA.

Epitopes	Sites	Outliers
N2_A	82, 83, 84, 86, 88, 89, 90, 187, 207, 208, 234, 236, 258, 259, 283, 284, 285, 286, 306, 307, 308, 309, 311, 357, 415, 416	–
N2_B	118, 143, 146, 147, 150, 151, 152, 153, 154, 156, 178, 406, 430, 431, 432, 433, 434, 437, 469	–
N2_C	195, 196, 197, 198, 199, 200, 218, 219, 220, 221, 222, 224, 244, 245, 246, 247, 248, 249, 250, 251, 253, 268, 273, 274, 276, 277	–
N2_D	292, 294, 295, 296, 326, 327, 328, 329, 331, 332, 333, 334, 339, 342, 343, 344, 345, 346, 347, 348, 358, 369, 370, 371, 384, 385, 390	358,384,385,390
N2_E	392, 394, 399, 400, 401, 402, 453, 454, 455, 456, 457, 458	–

Note: "–" means no outlier sites were identified for the corresponding epitope.
Abbreviation: NA=neuraminidase.

SUPPLEMENTARY TABLE 3. Vaccine strains included in each antigenic cluster.

Vac_strains	Accession number	Cluster
A/Port_chalmers/1/1973	EPI_ISL_20940	PC73
A/Victoria/3/1975	EPI_ISL_113968	PC73
A/Texas/1/1977	EPI_ISL_122019	TE77
A/Bangkok/1/1979	EPI_ISL_122020	TE77
A/Philippines/2/1982	EPI_ISL_76487	TE77
A/Leningrad/360/1986	EPI_ISL_124928	TE77
A/Shanghai/11/1987	EPI_ISL_114294	TE77
A/Sichuan/2/1987	EPI_ISL_125877	TE77
A/Beijing/353/1989	EPI_ISL_115769	BJ89
A/Guizhou/54/1989	EPI_ISL_124894	BJ89
A/Beijing/32/1992	EPI_ISL_22624	BJ89
A/Shangdong/9/1993	EPI_ISL_115410	BJ89
A/Johannesurg/33/1994	EPI_ISL_14284833	BJ89
A/Wuhan/359/1995	EPI_ISL_111269	WH95
A/Nanchang/933/1995	EPI_ISL_14284834	WH95
A/Sydney/5/1997	EPI_ISL_14284880	WH95
A/Moscow/10/1999	EPI_ISL_127595	MS99
A/Panama/2007/1999	EPI_ISL_174195	WH95
A/Fujian/411/2002	EPI_ISL_107711	MS99
A/Wyoming/03/2003	EPI_ISL_153570	MS99
A/Fujian/445/2003	EPI_ISL_127602	MS99
A/California/7/2004	EPI_ISL_21094	CA04
A/Wellington/01/2004	EPI_ISL_127603	CA04*
A/Newyork/55/2004	EPI_ISL_2402569	CA04
A/Hiroshima/52/2005	EPI_ISL_13228	CA04
A/Wisconsin/67/2005	EPI_ISL_10430	CA04
A/Jiangxi/donghu312/2006	EPI_ISL_20194	CA04

Continued

Vac_strains	Accession number	Cluster
A/Brisbane/10/2007	EPI_ISL_110723	PE09
A/Perth/16/2009	EPI_ISL_31913	PE09
A/Fujian-tongan/196/2009	EPI_ISL_99110	PE09
A/Victoria/361/2011	EPI_ISL_109762	PE09
A/Texas/50/2012	EPI_ISL_122006	PE09
A/Switzerland/9715293/2013	EPI_ISL_166859	PE09
A/Hong_kong/4801/2014	EPI_ISL_176512	PE09
A/Singapore/infimh-16-0019/2016	EPI_ISL_330262	SI16
A/Kansas/14/2017	EPI_ISL_312833	SI16
A/Switzerland/8060/2017	EPI_ISL_303951	SI16
A/Southaustralia/34/2019	EPI_ISL_17668123	SI16
A/Hong_kong/2671/2019	EPI_ISL_391201	SI16
A/Hongkong/45/2019	EPI_ISL_410589	SI16
A/Cambodia/e0826360/2020	EPI_ISL_1367566	SI16
A/Darwin/6/2021	EPI_ISL_18879343	SI16
A/Darwin/9/2021	EPI_ISL_16998754	SI16
A/Thailand/8/2022	EPI_ISL_18485009	SI16
A/Massachusetts/18/2022	EPI_ISL_16968012	SI16
A/Croatia/10136rv/2023	EPI_ISL_19085873	SI16
A/District_of_ columbia/27/2023	EPI_ISL_19175844	SI16

* Derived from even sampling.

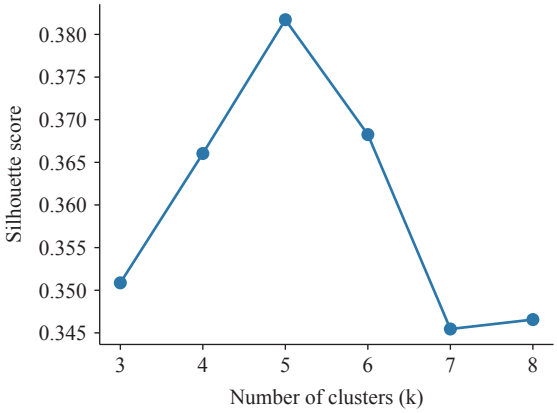

SUPPLEMENTARY FIGURE S1. Silhouette score curve for different values of k (number of epitopes).
Note: A higher score represents better clustering results.

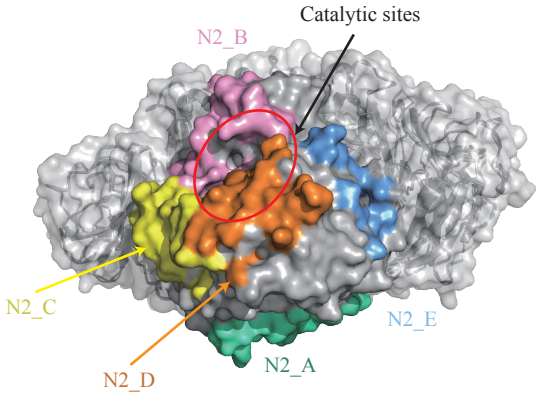

SUPPLEMENTARY FIGURE S2. Identified epitopes. Different colors indicate distinct epitopes.
Note: The red circle indicates catalytic sites. Epitopes are shown on only one chain of the tetramer.

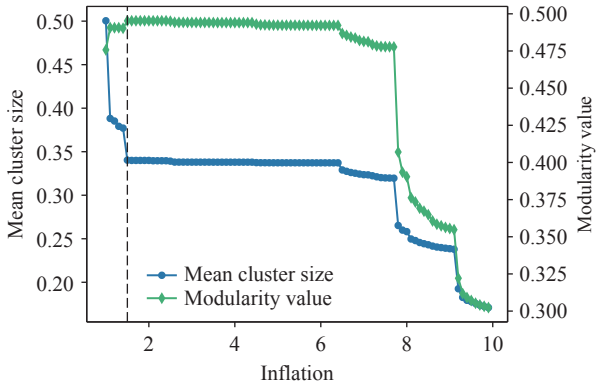

SUPPLEMENTARY FIGURE S3. Average cluster size and modularity curve.
Note: The blue line represents the mean cluster size (left y-axis). The green line represents modularity (right y-axis). The parameter corresponding to the first point in the first plateau period was selected, with higher modularity representing better clustering results. An inflation value of 1.5 for MCL was selected.

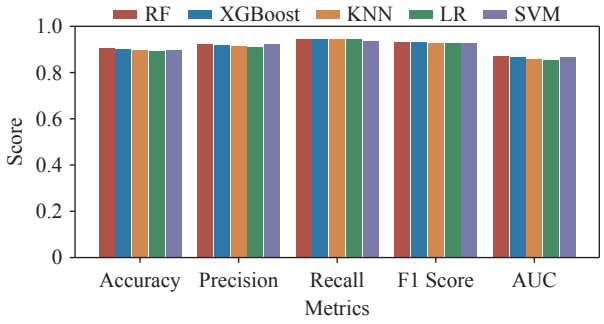

SUPPLEMENTARY FIGURE S4. Performance of different models on the training dataset based on 5-fold cross-validation.
Abbreviation: RF=random forest; XGBoost=extreme gradient boosting; KNN=K-nearest neighbors; LR=logistic regression; SVM=support vector machine; AUC=receiver operating characteristic area under the curve.

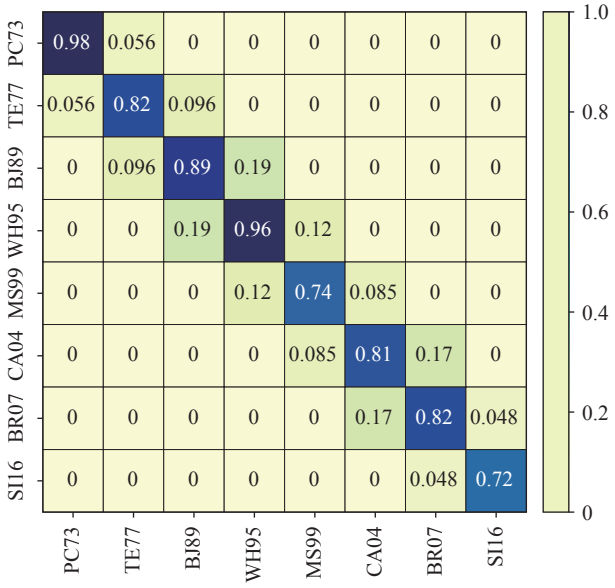

SUPPLEMENTARY FIGURE S5. Antigenic similarity proportion for eight antigenic clusters.
Note: The proportions were calculated based on all possible pairs within a cluster and between two clusters.

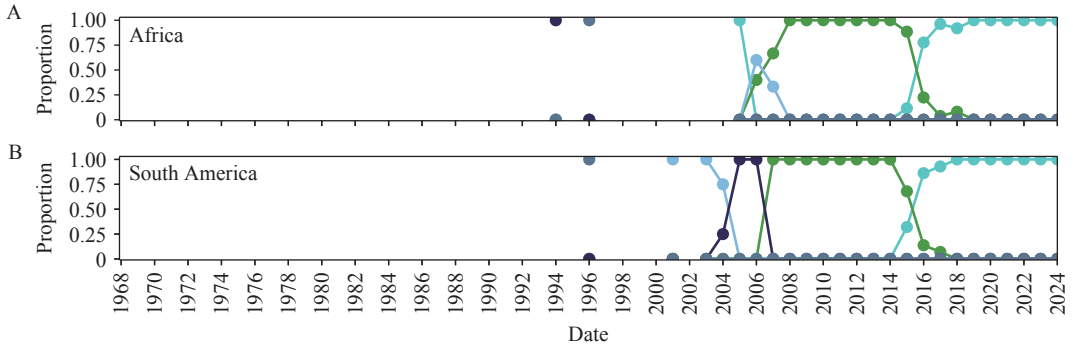

SUPPLEMENTARY FIGURE S6. Spatiotemporal distribution of even sampling for eight antigenic clusters in (A) Africa, and (B) South America.

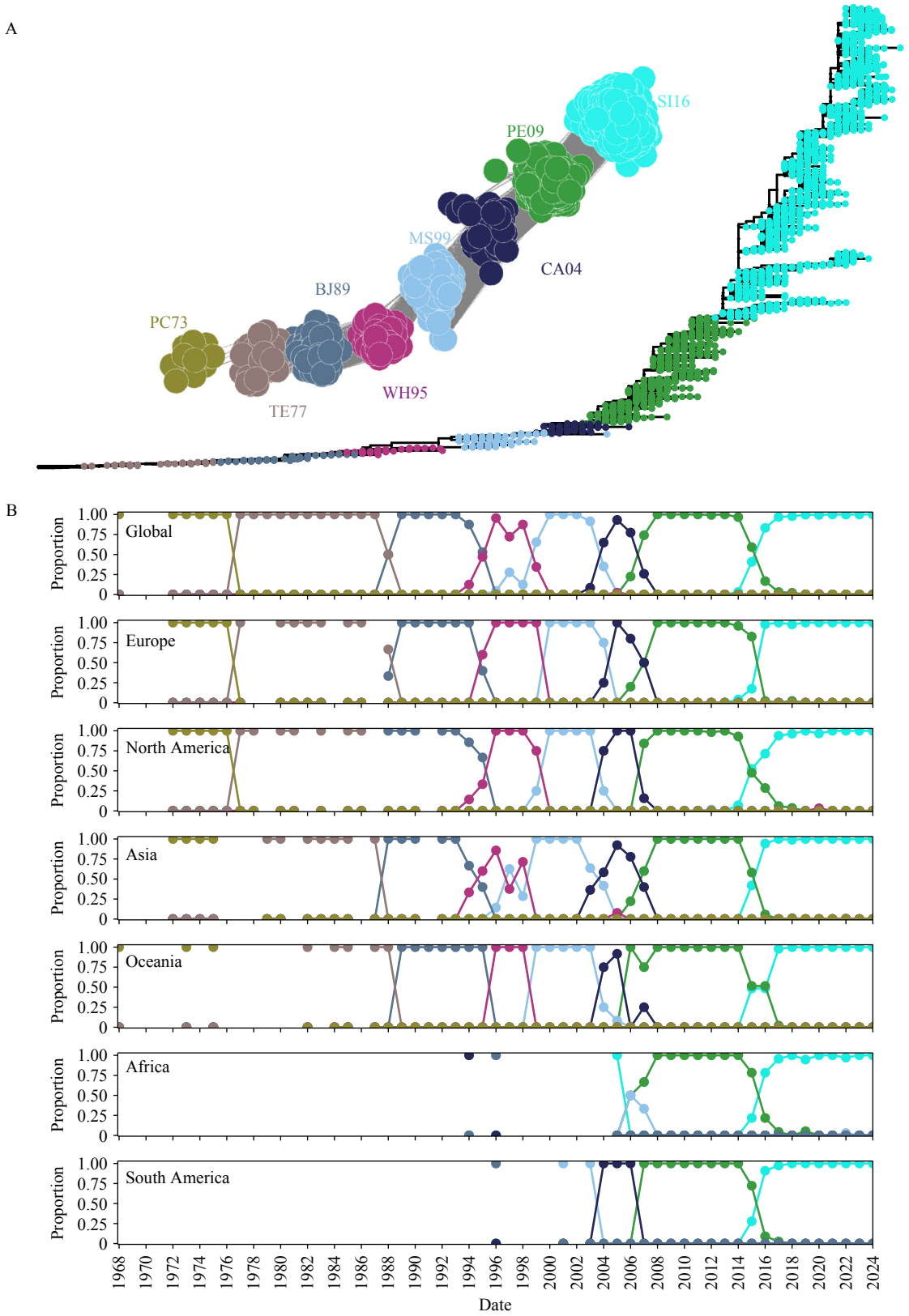

SUPPLEMENTARY FIGURE S7. Antigenic landscape of A/H3N2 NA from proportional sampling. (A) The ACNet and phylogenetic tree of representative sequences from eight major antigenic clusters; (B) Yearly spatiotemporal distribution of eight antigenic clusters.
Abbreviation: NA=neuraminidase; ACNet=antigenic correlation network.

REFERENCES

1. Catani JPP, Smet A, Ysenbaert T, Vuylsteke M, Bottu G, Mathys J, et al. The antigenic landscape of human influenza N2 neuraminidases from 2009 until 2017. eLife 2024;12:RP90782. https://doi.org/10.7554/eLife.90782.4.
2. Sandbulte MR, Westgeest KB, Gao J, Xu XY, Klimov AI, Russell CA, et al. Discordant antigenic drift of neuraminidase and hemagglutinin in H1N1 and H3N2 influenza viruses. Proc Natl Acad Sci USA 2011;108(51):20748 – 53. https://doi.org/10.1073/pnas.1113801108.
3. Gao J, Li X, Klenow L, Malik T, Wan HQ, Ye ZP, et al. Antigenic comparison of the neuraminidases from recent influenza A vaccine viruses and 2019–2020 circulating strains. npj Vaccines 2022;7(1):79. https://doi.org/10.1038/s41541-022-00500-1.
4. Schild GC, Oxford JS, Dowdle WR, Coleman M, Pereira MS, Chakraverty P. Antigenic variation in current influenza A viruses: evidence for a high frequency of antigenic 'drift' for the Hong Kong virus. Bull World Health Organ 1974;51(1):1-11. https://pubmed.ncbi.nlm.nih.gov/4218138/.
5. Kilbourne ED, Johansson BE, Grajower B. Independent and disparate evolution in nature of influenza A virus hemagglutinin and neuraminidase glycoproteins. Proc Natl Acad Sci USA 1990;87(2):786 – 90. https://doi.org/10.1073/pnas.87.2.786.

Review

Clade Ib Mpox Virus: How Can We Respond?

Lin Ai[1,&]; Xinyi Cui[2,&]; Yanqiu Zhou[1,#]

ABSTRACT

In recent years, mpox virus Clade Ib has emerged as a significant global public health threat due to its rapid transmission and potential for severe disease outcomes. This strain was first identified in the Democratic Republic of the Congo (DRC) in September 2023 and began spreading to neighboring African countries by July 2024. It was subsequently imported through international travel to 12 non-African countries across Asia, Europe, and the Americas. Clade Ib exhibits increased transmissibility, and current data suggest that infections may lead to more severe symptoms, with higher risks of severe illness and mortality, particularly among vulnerable populations such as children, pregnant individuals, and immunocompromised groups (e.g., people living with HIV/AIDS). Epidemiologically, Clade Ib primarily spreads through sexual contact, close household contact, and healthcare-related exposure. This review aims to provide an overview of the current understanding of mpox virus Clade Ib, including its genetic characteristics, epidemiological patterns, and prevention and control strategies. Additionally, it discusses the strategies and interventions needed to address this emerging threat.

The mpox virus (MPXV) comprises two lineages: Clade I (Central African/Congo Basin strain) and Clade II (West African strain) (*1*), which have traditionally been associated with zoonotic transmission and limited human-to-human spread (*2*). The 2022–2023 global Clade II outbreak marked a significant shift, representing the first international emergence of MPXV, predominantly affecting male-to-male sexual networks in Europe and the Americas (*3*). Concurrently, the emergence of the Clade Ib variant in the Democratic Republic of Congo in 2023 triggered a substantial surge in Clade I infections across Africa (*4*–*5*). Following the World Health Organization (WHO)'s declaration of a public health emergency in August 2024 (*6*), intensified research on Clade Ib MPXV has become imperative to address critical knowledge gaps in viral evolution, outbreak prediction, and development of effective countermeasures. These research efforts are vital for enhancing global surveillance systems and optimizing containment strategies against MPXV dissemination.

The Harm of Mpox Virus Clade Ib to Human Health

Following the decline of Clade II, Central Africa's forest zones have experienced rising Clade I prevalence linked to zoonotic spillover and intrahousehold transmission (*7*). Clade Ib strains exhibit heightened virulence with a case fatality ratio (CFR) of 5.3% as of May 2024, characterized by distinctive clinical manifestations including disseminated eruptions, pharyngitis, persistent fever, and lymphadenopathy (*8*). Surveillance data indicate expanding geographic spread across 23 of 26 provinces in the Democratic Republic of Congo, disproportionately affecting pediatric populations (under 15 years) with severe outcomes (*6*). The 2023 epidemiological shift reveals novel transmission clusters in previously unaffected regions, underscoring intensified human-to-human spread alongside more than 700 suspected infections reported in 2024 (*9*).

The Genetic Characteristics of Mpox Virus Clade Ib

Genomic characterization has identified a distinct Clade Ib variant in South Kivu, originating from independent zoonotic transmission (*3*). While Clades I and II share high conservation (99.3% identity), accurate lineage differentiation requires insertion/deletion (INDEL) profiling (*10*). Although phylogenetically grouped within Clade I, these strains lack the CDC-endorsed diagnostic target due to a 1,114-nucleotide deletion (OPG032 loss), which compromises PCR reliability (*5*). Significant evolutionary divergence is evident between subclades, with Clade Ib exhibiting 16.7% APOBEC3-driven

SNPs compared to just 0.3% in Clade Ia, suggesting distinct evolutionary trajectories (*11*). The deletion of the C3L gene in Clade Ib, a key Clade I marker, presents critical diagnostic challenges that may result in false-negative results, particularly during periods of Clade II co-circulation (*5*,*10*,*12*).

Epidemiological Characteristics of Mpox Virus Clade Ib

Epidemic regions: Clade Ib emerged in South Kivu, Democratic Republic of Congo (September 2023) as a phylogenetically distinct lineage (*12*), rapidly expanding to 14 health zones within 11 months and crossing borders into four neighboring nations (Burundi, Rwanda, Uganda, Kenya) by August 2024 (*13*). The World Health Organization reissued its mpox Public Health Emergency of International Concern following this accelerated transnational spread, with travel-associated cases subsequently reported in Sweden (*14*) and Thailand (*15*) in August 2024. By autumn, autochthonous transmission was documented in India (September) (*16*), Germany (October) (*17*), England (October/November) (*18*–*19*), the United States (November) (*20*), and Brazil (November) (*21*), demonstrating Clade Ib's significant global dispersal capacity despite ongoing questions regarding its transmissibility.

Transmission route: Genomic epidemiology reveals Clade Ib's sustained human-to-human transmission through host-adaptive mutations (*12*), contrasting with Clade Ia's predominantly zoonotic and household transmission patterns (*22*). The absence of a defined core transmission group — combined with unsubstantiated associations between sexual orientation and transmission risk — creates potential for stigmatization and undermines surveillance effectiveness in non-endemic regions (*12*,*23*). Clade Ib demonstrates distinct transmission dynamics from Clade IIb, which primarily affects men who have sex with men (MSM) populations (*23*). In the Democratic Republic of Congo, Clade Ib infections show a demographically balanced sex distribution, with 72% [95% confidence interval (*CI*): 65%, 78%] linked to sexual networks, disproportionately affecting adolescents (15–19 years) and young adults (20–24 years), including sex workers (*23*). While sexual contact frequency significantly increases infection risk [odds ratio (*OR*)=3.4, $P<0.01$], no specific sexual practices or orientations show significant association (*12*), challenging assumptions that conflate particular intimate behaviors with Clade Ib transmission.

Susceptible population: Epidemiological data confirm two distinct Clade Ib outbreak patterns in the DRC: 1) clusters among adult female sex workers (*24*), and 2) pediatric populations exhibiting heightened susceptibility and mortality (*25*). Surveillance records from 2024 document over 7,000 suspected cases with a case fatality ratio of 5.3%, with children aged ≤15 years constituting 67% of cases and 84% of fatalities (*9*). Infants under 5 years demonstrate a fourfold higher mortality risk compared to older age groups (*26*), highlighting household and community transmission as the predominant infection pathway.

Detection on Clade Ib Mpox

The high genomic conservation between MPXV Clades I and II (>99% nucleotide identity in core regions) and broad *Orthopoxvirus* homology (>90%) presents significant challenges for lineage-specific assay development (*10*). Phylogenetic convergence necessitates structural variation analysis, with validated INDEL polymorphisms serving as critical Clade-discriminatory markers (*10*).

PCR remains the gold standard for MPXV confirmation. CDC-endorsed real-time PCR assays effectively distinguish Clades I/II from other *Orthopoxvirus* species (*27*–*28*), though some C3L-adjacent assays demonstrate uncertain reliability for Clade Ib differentiation (*29*). Recent advancements include a Clade Ib-specific TaqMan probe targeting C3L deletions, which enhances transmission network tracking in non-endemic regions (*30*).

Whole genome sequencing (WGS) analyses of Clade Ib strains have revealed seven hotspot mutations (C9L-B21R) and consistent OPG032 (D14L) deletions, establishing a novel subgroup (VI) within Clade I through phylogenetic clustering (*31*). These findings underscore the necessity for enhanced genomic surveillance in endemic regions.

Serological surveillance complements molecular diagnostics by detecting subclinical infections. African studies demonstrate 6.3% *Orthopoxvirus* IgG seropositivity in asymptomatic populations (*32*), while 2022 outbreak data revealed 10.2% asymptomatic transmission-capable cases (*33*). Recent investigations identified 8.1% (91/1,119) suspected undiagnosed infections through serology (*34*). Modern immunoblot techniques improve Clade-specific antibody detection, overcoming cross-reactivity challenges inherent to conventional enzyme-linked immunosorbent assay (ELISA) (*35*). Neutralization assays differentiate

vaccine-derived from natural infection antibodies, which is critical for epidemiological mapping (*36*–*37*). Integrated sero-genomic surveillance could refine pandemic models by quantifying gaps in symptom-based reporting systems.

Prevention and Control Measures

Effective prevention and control of MPXV, particularly Clade Ib, requires a comprehensive strategy encompassing enhanced surveillance, public education, and isolation protocols (*38*). Robust surveillance systems are essential for early detection and rapid outbreak response (*39*). Healthcare settings should implement rapid diagnostic testing, complemented by targeted public health campaigns that educate high-risk populations — including healthcare workers and individuals in close contact with infected animals — about transmission mechanisms, symptom recognition, and preventive measures (*24*,*40*).

Vaccines

Vaccination remains the cornerstone of mpox prevention, particularly given the high pediatric mortality rates associated with Clade Ib infections (*41*). Three live-attenuated smallpox vaccines are currently available:

Routine vaccines: MVA-BN (JYNNEOS®/Imvamune®/Imvanex®). This non-replicating vaccine is globally approved and safe for immunocompromised individuals, pregnant women, and those with dermatologic conditions. It requires a two-dose regimen with a 4-week interval and demonstrated 62%–85% efficacy during the 2022 outbreaks, significantly reducing disease severity (*42*–*44*).

LC16m8. This low-replicating strain developed in Japan confers 100% protection in non-human primates (NHPs) against Clade I MPXV (*45*). It induces neutralizing antibodies with 70% seroconversion (*46*) and exhibits only mild side effects, including fever and lymphadenopathy (*47*). Over 90,000 individuals, including 50,000 children, have been vaccinated with LC16m8 without significant safety concerns (*48*).

ACAM2000. This replication-competent vaccine is authorized for emergency use but contraindicated in immunocompromised individuals due to risks of myopericarditis. It served as the primary mpox vaccine in the U.S. until 2019 (*49*–*50*).

Next-generation vaccines: Several innovative vaccine platforms are currently under development for mpox prevention. Quadrivalent mRNA vaccines (e.g., mRNA-A/B-LNP) targeting A29L, A35R, M1R, and B6R have demonstrated robust neutralizing antibody production and T-cell responses in murine models (*51*).

Multivalent mRNA vaccines such as Mpoxac-097 induce protective CD8+ T-cell responses against vaccinia virus (VACV) challenge, representing a promising advancement in orthopoxvirus immunization (*52*).

Additional candidates include encapsulated mRNA vaccines targeting A35R/M1R antigens and multicomponent formulations, which elicit Th1-biased immune responses with efficacy comparable to traditional vaccines in preclinical murine studies (*53*–*54*).

Drugs and Clinical Treatment

Drugs: Tecovirimat, a broad-spectrum antiviral, inhibits the p37 protein (encoded by the C17L gene in VARV), a conserved *Orthopoxvirus* target essential for viral envelope formation and pathogenicity (*55*). Approved by the U.S. FDA in 2018 for smallpox treatment, it effectively blocks the production of enveloped virions across the *Orthopoxvirus* genus.

Brincidofovir, an oral cidofovir analog approved in 2021 for smallpox, offers reduced nephrotoxicity compared to its injectable predecessor (*56*). Both agents inhibit viral replication through DNA polymerase inhibition (*57*).

Clinical treatment: Interim analyses from the National Institute of Allergy and Infectious Diseases (NIAID)-sponsored PALM007 (NCT05559099) and STOMP (NCT05534984) trials demonstrated tecovirimat's safety but found no efficacy in accelerating lesion resolution compared to placebo. PALM007, which enrolled hospitalized adults and children receiving high-quality supportive care, reported 1.7% mortality (historically ≥3.6%), attributing improved outcomes to enhanced supportive measures rather than tecovirimat. Similarly, STOMP's double-blinded cohort (mild-to-moderate cases, 2:1 allocation) showed no significant lesion or pain reduction with tecovirimat. Both trials confirmed the drug's tolerability (no serious adverse events) but demonstrated limited clinical benefit in immunocompetent patients with low-severity disease (*58*). Subgroup analyses are ongoing for immunocompromised individuals, patients with advanced HIV coinfection, and those receiving early treatment initiation.

Brincidofovir, FDA-approved for smallpox across all age groups, has demonstrated efficacy against *Orthopoxvirus* in both in vitro and animal studies, though human data specific to MPXV remain limited (*58*).

Challenges and Future Prospects

The emergence of MPXV Clade Ib in China presents significant public health challenges alongside strategic opportunities. Key challenges include its potential to escape existing vaccines, which could compromise immunization strategies and outbreak containment efforts, and its elevated mutation rate, necessitating continuous real-time genomic surveillance and adaptive public health responses. Conversely, this emergence creates opportunities to accelerate development of Clade Ib-specific vaccines and therapeutics while strengthening cross-border collaborations for coordinated resource mobilization. The escalating transmission risks underscore the urgent need for targeted health communication strategies to enhance community-level outbreak preparedness.

CONCLUSION

In summary, MPXV Clade Ib has emerged as a significant strain with substantial impact on disease epidemiology. It poses a considerable public health threat due to its enhanced transmission potential and the severity of illness it causes. The strain's rapid geographic spread, coupled with its distinct clinical presentation and higher case fatality ratio, underscores the urgent need for coordinated global surveillance, targeted prevention strategies, and continued development of effective vaccines and therapeutics. As international cases continue to emerge, strengthening cross-border collaboration and implementing evidence-based public health measures remain essential to mitigate the impact of this evolving pathogen.

Conflicts of interest: No conflicts of interest.

Funding: Supported by Research on Genetic Evolution Characteristics and Key Techniques for Tracing of Highly Pathogenic Viruses (2023YFC2605602) , the key research project of Three-Year Initiative Plan for Strengthening Public Health System Construction in Shanghai (2023-2025) (GWVI-3), Three-Year Initiative Plan for Strengthening Public Health System Construction in Shanghai (2023-2025) Key Discipline Project (GWVI-11.1-12), Key Discipline- Infectious Diseases of Three-year Action Program of Shanghai Municipality for Strengthening the Construction of Public Health System (2023–2025) (GWVI-11.1-01), the Key Discipline Program on Public Health System Construction of Shanghai (GWVI-11.1-15), Shanghai Municipal Science and Technology Major Project (ZD2021CY001).

doi: 10.46234/ccdcw2025.165

[#] Corresponding author: Yanqiu Zhou, zhouyanqiu@scdc.sh.cn.

[1] Institute of Microbiology Laboratory, Shanghai Municipal Center for Disease Control and Prevention, Shanghai, China; [2] Shanghai Academy of Preventive Medicine, Shanghai, China.
[&] Joint first authors.

Submitted: December 27, 2024
Accepted: April 18, 2025
Issued: July 18, 2025

REFERENCES

1. Gessain A, Nakoune E, Yazdanpanah Y. Monkeypox. N Engl J Med 2022;387(19):1783 – 93. https://doi.org/10.1056/NEJMra2208860.
2. Ježek Z, Grab B, Szczeniowski MV, Paluku KM, Mutombo M. Human monkeypox: secondary attack rates. Bull World Health Organ 1988;66 (4):465 – 70.
3. Gao L, Shi Q, Dong X, Wang M, Liu Z, Li Z. Mpox, Caused by the MPXV of the Clade IIb Lineage, Goes Global. Trop Med Infect Dis 2023;8(2):76 https://doi.org/10.3390/tropicalmed8020076.
4. Centers for Disease Control and Prevention (CDC). 2022-2023 Mpox outbreak global map. https://www.cdc.gov/poxvirus/mpox/response/2022/world-map.html. [2024-7-20].
5. Masirika LM, Udahemuka JC, Schuele L, Ndishimye P, Otani S, Mbiribindi JB, et al. Ongoing mpox outbreak in Kamituga, South Kivu Province, associated with monkeypox virus of a novel clade I sub-lineage, Democratic Republic of the Congo, 2024. Euro Surveill 2024;29(11):2400106. https://doi.org/10.2807/1560-7917.ES.2024.29.11.2400106.
6. World Health Organization (WHO). WHO Re-Declares Monkeypox as a Public Health Emergency of International Concern. https://www.who.int/news/item/14-08-2024-who-director-general-declares-mpox-outbreak-a-public-health-emergency-of-international-concern. [2024-8-14].
7. Djuicy DD, Sadeuh-Mba SA, Bilounga CN, Yonga MG, Tchatchueng-Mbougua JB, Essima GD, et al. Concurrent clade I and clade II monkeypox virus circulation, cameroon, 1979-2022. Emerg Infect Dis 2024;30(3):432 – 43. https://doi.org/10.3201/eid3003.230861.
8. Charniga K, McCollum AM, Hughes CM, Monroe B, Kabamba J, Lushima RS, et al. Updating reproduction number estimates for mpox in the Democratic Republic of Congo using surveillance data. Am J Trop Med Hyg 2024;110(3):561 – 8. https://doi.org/10.4269/ajtmh.23-0215.
9. Titanji BK, Hazra A, Zucker J. Mpox clinical presentation, diagnostic approaches, and treatment strategies: a review. JAMA 2024;332(19): 1652 – 62. https://doi.org/10.1001/jama.2024.21091.
10. Li Y, Zhao H, Wilkins K, Hughes C, Damon IK. Real-time PCR assays for the specific detection of monkeypox virus west African and Congo Basin strain DNA. J Virol Methods 2010;169(1):223 – 7. https://doi.org/10.1016/j.jviromet.2010.07.012.

11. Kinganda-Lusamaki E, Amuri-Aziza A, Fernandez-Nuñez N, Makangara-Cigolo JC, Pratt C, Vakaniaki EH, et al. Clade I mpox virus genomic diversity in the Democratic Republic of the Congo, 2018-2024: predominance of zoonotic transmission. Cell 2025;188(1):4 – 14.e6. https://doi.org/10.1016/j.cell.2024.10.017.
12. Vakaniaki EH, Kacita C, Kinganda-Lusamaki E, O'Toole Á, Wawina-Bokalanga T, Mukadi-Bamuleka D, et al. Sustained human outbreak of a new MPXV clade I lineage in eastern Democratic Republic of the Congo. Nat Med 2024;30(10):2791 – 5. https://doi.org/10.1038/s41591-024-03130-3.
13. Marty AM, Beÿ CK, Koenig KL. 2024 Mpox outbreak: A rapidly evolving public health emergency of international concern: Introduction of an Updated Mpox Identify-Isolate-Inform (3I) Tool. One Health 2024;19:100927 https://doi.org/10.1016/j.onehlt.2024.100927.
14. Treutiger CJ, Filén F, Rehn M, Aarum J, Jacks A, Gisslén M, et al. First case of mpox with monkeypox virus clade Ib outside Africa in a returning traveller, Sweden, August 2024: public health measures. Euro Surveill 2024;29(48):2400740. https://doi.org/10.2807/1560-7917.ES.2024.29.48.2400740.
15. Wappes J. More global mpox spread as clade 1b confirmed in Thailand, the 2nd case outside Africa. CIDRAP. 2024. https://www.cidrap.umn.edu/mpox/more-global-mpox-spread-clade-1b-confirmed-thailand-2nd-case-outside-africa. [2024-9-3].
16. Sah S, Dhandh YK, Mehta R, Singh MP, Bushi G, Shabil M, et al. First imported clade 1b mpox case in India: implications for travel medicine and public health surveillance. Travel Med Infect Dis 2024;62:102766. https://doi.org/10.1016/j.tmaid.2024.102766.
17. Nzoyikorera N, Nduwimana C, Schuele L, Nieuwenhuijse DF, Koopmans M, Otani S, et al. monkeypox clade Ib virus introduction into Burundi: first findings, July to mid-August 2024. Euro Surveill 2024;29(42):2400666. https://doi.org/10.2807/1560-7917.ES.2024.29.42.2400666.
18. Kmietowicz Z. UK confirms first case of clade Ib mpox. BMJ 2024;387:q2406. https://doi.org/10.1136/bmj.q2406.
19. Iacobucci G. UK reports two further cases of clade Ib mpox. BMJ 2024;387:q2442. https://doi.org/10.1136/bmj.q2442.
20. Mahase E. Mpox: US reports first clade Ib case as campaigners call for cheaper tests. BMJ 2024;387:q2576. https://doi.org/10.1136/bmj.q2576.
21. Martins-Filho PR, Carvalho TA, Rodrigues SSA, de Sousa DS, Araújo FWC, Tenório MDL, et al. Confronting mpox in Brazil amid global spread of clade Ib. Lancet Reg Health Am 2024;40:100917. https://doi.org/10.1016/j.lana.2024.100917.
22. Whitehouse ER, Bonwitt J, Hughes CM, Lushima RS, Likafi T, Nguete B, et al. Clinical and epidemiological findings from enhanced monkeypox surveillance in Tshuapa Province, Democratic Republic of the Congo during 2011-2015. J Infect Dis 2021;223(11):1870 – 8. https://doi.org/10.1093/infdis/jiab133.
23. Allan-Blitz LT, Gandhi M, Adamson P, Park I, Bolan G, Klausner JD. A position statement on mpox as a sexually transmitted disease. Clin Infect Dis 2023;76(8):1508 – 12. https://doi.org/10.1093/cid/ciac960.
24. Decousser JW, Keita-Perse O, Aho Glele LS, Baron R, Carre Y, Cassier P, et al. Transmission pathways and personal protective equipment requirement for mpox clade Ib lineage: nothing new on this front. J Hosp Infect 2025;156:125 – 7. https://doi.org/10.1016/j.jhin.2024.10.018.
25. Brosius I, Vakaniaki EH, Mukari G, Munganga P, Tshomba JC, De Vos E, et al. Epidemiological and clinical features of mpox during the clade Ib outbreak in South Kivu, Democratic Republic of the Congo: a prospective cohort study. Lancet. 2025;405(10478):547 – 559 https://doi.org/10.1016/S0140-6736(25)00047-9.
26. Yinka-Ogunleye A, Dalhat M, Akinpelu A, Aruna O, Garba F, Ahmad A, et al. Mpox (monkeypox) risk and mortality associated with HIV infection: a national case-control study in Nigeria. BMJ Glob Health 2023;8(11):e013126 https://doi.org/10.1136/bmjgh-2023-013126.
27. de Vries HJ, Götz HM, Bruisten S, van der Eijk AA, Prins M, Oude Munnink BB, et al. Mpox outbreak among men who have sex with men in Amsterdam and Rotterdam, the Netherlands: no evidence for undetected transmission prior to May 2022, a retrospective study. Euro Surveill 2023;28(17):2200869. https://doi.org/10.2807/1560-7917.ES.2023.28.17.2200869.
28. Liesenborghs L, Coppens J, Van Dijck C, Brosius I, De Baetselier I, Vercauteren K, et al. No evidence for clade I monkeypox virus circulation, Belgium. Emerg Infect Dis 2024;30(2):402. https://doi.org/10.3201/eid3002.231746.
29. Huo ST, Chen YD, Lu RJ, Zhang ZX, Zhang GQ, Zhao L, et al. Development of two multiplex real-time PCR assays for simultaneous detection and differentiation of monkeypox virus IIa, IIb, and I clades and the B. 1 lineage. Biosaf Health 2022;4(6):392 – 8. https://doi.org/10.1016/j.bsheal.2022.10.005.
30. Schuele L, Masirika LM, Udahemuka JC, Siangoli FB, Mbiribindi JB, Ndishimye P, et al. Real-time PCR assay to detect the novel clade Ib monkeypox virus, September 2023 to May 2024. Euro Surveill 2024;29(32):2400486. https://doi.org/10.2807/1560-7917.ES.2024.29.32.2400486.
31. Masirika LM, Kumar A, Dutt M, Ostadgavahi AT, Hewins B, Nadine MB, et al. Complete genome sequencing, annotation, and mutational profiling of the novel clade I human mpox virus, Kamituga strain. J Infect Dev Ctries 2024;18(4):600 – 8. https://doi.org/10.3855/jidc.20136.
32. Guagliardo SAJ, Monroe B, Moundjoa C, Athanase A, Okpu G, Burgado J, et al. Asymptomatic orthopoxvirus circulation in humans in the wake of a monkeypox outbreak among chimpanzees in Cameroon. Am J Trop Med Hyg 2020;102(1):206 – 12. https://doi.org/10.4269/ajtmh.19-0467.
33. Satapathy P, Mohanty P, Manna S, Shamim MA, Rao PP, Aggarwal AK, et al. Potentially asymptomatic infection of monkeypox virus: a systematic review and meta-analysis. Vaccines (Basel) 2022;10(12):2083. https://doi.org/10.3390/vaccines10122083.
34. Marcus U, Michel J, Lunchenkov N, Beslic D, Treindl F, Surtees R, et al. A seroprevalence study indicates a high proportion of clinically undiagnosed MPXV infections in men who have sex with men in Berlin, Germany. BMC Infect Dis 2024;24(1):1153. https://doi.org/10.1186/s12879-024-10066-z.
35. Minhaj FS, Singh V, Cohen SE, Townsend MB, Scott H, Szumowski J, et al. Prevalence of undiagnosed monkeypox virus infections during global mpox outbreak, United States, June-September 2022. Emerg Infect Dis 2023;29(11):2307 – 14. https://doi.org/10.3201/eid2911.230940.
36. Hubert M, Guivel-Benhassine F, Bruel T, Porrot F, Planas D, Vanhomwegen J, et al. Complement-dependent mpox-virus-neutralizing antibodies in infected and vaccinated individuals. Cell Host Microbe 2023;31(6):937 – 48.e4. https://doi.org/10.1016/j.chom.2023.05.001.
37. Marchi S, Piccini G, Cantaloni P, Guerrini N, Zannella R, Coluccio R, et al. Evaluation of monkeypox- and vaccinia-virus neutralizing antibodies before and after smallpox vaccination: a sero-epidemiological study. J Med Virol 2024;96(6):e29728. https://doi.org/10.1002/jmv.29728.
38. Ndembi N, Abdool Karim SS. Africa aims to avert an mpox pandemic. Science 2024;386(6717):7. https://doi.org/10.1126/science.adt4793.
39. Mukadi-Bamuleka D, Kinganda-Lusamaki E, Mulopo-Mukanya N, Amuri-Aziza A, O'Toole Á, Modadra-Madakpa B, et al. First imported cases of MPXV clade Ib in Goma, Democratic Republic of the Congo: implications for global surveillance and transmission dynamics. medRxiv 2024;24313188. http://dx.doi.org/10.1101/2024.09.12.24313188.
40. Adebisi YA, Ezema SM, Bolarinwa O, Bassey AE, Ogunkola IO. Sex workers and the mpox response in Africa. J Infect Dis 2024;230(4):786 – 8. https://doi.org/10.1093/infdis/jiae435.
41. Prompetchara E, Ketloy C, Khawsang C, Ruxrungtham K, Palaga T. Mpox global health emergency: insights into the virus, immune responses, and advancements in vaccines PART I: insights into the virus and immune responses. Asian Pac J Allergy Immunol 2024;42(3):181 – 90. https://doi.org/10.12932/AP-111024-1945.
42. Navarro C, Lau C, Buchan SA, Burchell AN, Nasreen S, Friedman L, et

al. Effectiveness of modified vaccinia Ankara-Bavarian Nordic vaccine against mpox infection: emulation of a target trial. BMJ 2024;386: e078243 https://doi.org/10.1136/bmj-2023-078243.
43. Grabenstein JD, Hacker A. Vaccines against mpox: MVA-BN and LC16m8. Expert Rev Vaccines 2024;23(1):796 – 811. https://doi.org/10.1080/14760584.2024.2397006.
44. Mason LMK, Betancur E, Riera-Montes M, Lienert F, Scheele S. MVA-BN vaccine effectiveness: a systematic review of real-world evidence in outbreak settings. Vaccine 2024;42(26):126409. https://doi.org/10.1016/j.vaccine.2024.126409.
45. Zuiani A, Dulberger CL, De Silva NS, Marquette M, Lu YJ, Palowitch GM, et al. A multivalent mRNA monkeypox virus vaccine (BNT166) protects mice and macaques from orthopoxvirus disease. Cell 2024;187 (6):1363 – 73.e12. https://doi.org/10.1016/j.cell.2024.01.017.
46. Morino E, Mine S, Tomita N, Uemura Y, Shimizu Y, Saito S, et al. Mpox neutralizing antibody response to LC16m8 vaccine in healthy adults. NEJM Evid 2024;3(3):EVIDoa2300290. https://doi.org/10.1056/EVIDoa2300290.
47. Tomita N, Terada-Hirashima J, Uemura Y, Shimizu Y, Iwasaki H, Yano R, et al. An open-label, non-randomized study investigating the safety and efficacy of smallpox vaccine, LC16, as post-exposure prophylaxis for mpox. Hum Vaccin Immunother 2023;19(2):2242219 https://doi.org/10.1080/21645515.2023.2242219.
48. Okumura N, Ishikane M, Ujiie M, Ohmagari N. "Take" after LC16m8 for mpox. Int J Infect Dis 2023;134:290 – 1. https://doi.org/10.1016/j.ijid.2023.07.005.
49. Kandeel M, Morsy MA, Abd El-Lateef HM, Marzok M, El-Beltagi HS, Al Khodair KM, et al. Efficacy of the modified vaccinia Ankara virus vaccine and the replication-competent vaccine ACAM2000 in monkeypox prevention. Int Immunopharmacol 2023;119:110206. https://doi.org/10.1016/j.intimp.2023.110206.
50. Katamesh BE, Madany M, Labieb F, Abdelaal A. Monkeypox pandemic containment: does the ACAM2000 vaccine play a role in the current outbreaks? Expert Rev Vaccines 2023;22(1):366-8. http://dx.doi.org/10.1080/14760584.2023.2198600.
51. Sang Y, Zhang Z, Liu F, Lu HT, Yu CX, Sun HS, et al. Monkeypox virus quadrivalent mRNA vaccine induces immune response and protects against vaccinia virus. Signal Transduct Target Ther 2023;8(1): 172. https://doi.org/10.1038/s41392-023-01432-5.
52. Fang ZH, Monteiro VS, Renauer PA, Shang XB, Suzuki K, Ling XY, et al. Polyvalent mRNA vaccination elicited potent immune response to monkeypox virus surface antigens. Cell Res 2023;33(5):407 – 10. https://doi.org/10.1038/s41422-023-00792-5.
53. Ye TX, Zhou JG, Guo C, Zhang KY, Wang YP, Liu YH, et al. Polyvalent mpox mRNA vaccines elicit robust immune responses and confer potent protection against vaccinia virus. Cell Rep 2024;43(6): 114269. https://doi.org/10.1016/j.celrep.2024.114269.
54. Zhang RR, Wang ZJ, Zhu YL, Tang W, Zhou C, Zhao SQ, et al. Rational development of multicomponent mRNA vaccine candidates against mpox. Emerg Microbes Infect 2023;12(1):2192815. https://doi.org/10.1080/22221751.2023.2192815.
55. Yang G, Pevear DC, Davies MH, Collett MS, Bailey T, Rippen S, et al. An orally bioavailable antipoxvirus compound (ST-246) inhibits extracellular virus formation and protects mice from lethal orthopoxvirus challenge. J Virol 2005;79(20):13139 – 49. https://doi.org/10.1128/JVI.79.20.13139-13149.2005.
56. Chittick G, Morrison M, Brundage T, Nichols WG. Short-term clinical safety profile of brincidofovir: a favorable benefit-risk proposition in the treatment of smallpox. Antiviral Res 2017;143:269 – 77. https://doi.org/10.1016/j.antiviral.2017.01.009.
57. Lanier R, Trost L, Tippin T, Lampert B, Robertson A, Foster S, et al. Development of CMX001 for the treatment of poxvirus infections. Viruses 2010;2(12):2740 – 62. https:// https://doi.org/10.3390/v2122740.
58. National Institutes of Health (NIH). NIH Study Finds Tecovirimat Was Safe but Did Not Improve Mpox Resolution or Pai. https://www.nih.gov/news-events/news-releases/nih-study-finds-tecovirimat-was-safe-did-not-improve-mpox-resolution-or-pain. [2024-12-10]

Notes from the Field

A Case of Psittacosis — Putian City, Fujian Province, China, April 2025

Zhiwei Zeng[1]; Tengwei Han[1]; Lingqiong Huang[1]; Zi Lin[2]; Weijun Liu[1]; Jing Liu[1]; Shenggen Wu[1]; Fangzhen Xiao[1,#]

On April 25, 2025, a case of psittacosis was identified in Putian City, Fujian Province. The patient was a 72-year-old female farmer who developed symptoms on April 1, 2025. Her primary clinical manifestations included cough, expectoration, dizziness, and shortness of breath. On April 3, 2025, the patient's condition deteriorated and was accompanied by fever peaking at 39.3 °C. She received symptomatic treatment at a county hospital. Due to further deterioration of her condition on April 5, 2025, she was transferred to a municipal hospital and admitted to the Emergency Intensive Care Unit (EICU) with severe pneumonia. During hospitalization, she received anti-infection treatment with doxycycline and moxifloxacin. By April 25, 2025, the patient's symptoms had improved significantly, and she was subsequently discharged from the hospital.

The patient had constructed a poultry enclosure adjacent to her newly built residence, housing eight chickens and ducks. She maintained daily contact with these birds without implementing protective measures and had no history of slaughtering poultry. Given her frequent and prolonged exposure to the birds combined with limited travel outside her home, infection through inhalation of aerosolized particles from contaminated poultry excreta represented the most probable transmission route. Notably, despite similar poultry contact, the patient's family members remained asymptomatic throughout the investigation period.

Chlamydia psittaci (*C. psittaci*) was identified in the patient's alveolar lavage fluid through targeted next-generation sequencing (NGS) testing for respiratory pathogens on April 11, 2025. Concurrently, the major outer membrane protein A (ompA) gene of *C. psittaci* was detected in both poultry feces and cage wipe specimens using real-time PCR and nested PCR (*1*). Sequence analysis revealed that the *C. psittaci* genes detected from the poultry feces and cage wipe specimens were identical to those identified in the patient, demonstrating 100% homology with a strain previously isolated from a patient in Shandong Province (accession number MZ345290) (*1*).

Psittacosis is a zoonotic disease caused by *C. psittaci* (*2*). Human infection typically occurs through direct contact with infected poultry or birds, as well as exposure to their contaminated feces or secretions (*3*). An increasing number of psittacosis cases have been documented worldwide (*3–5*), highlighting the growing recognition of this pathogen's clinical significance. Nevertheless, *C. psittaci* pneumonia accounts for only approximately 1.03% of community-acquired pneumonia cases (*6*), suggesting that numerous psittacosis infections remain underdiagnosed or misdiagnosed in clinical practice. Consequently, for pneumonia cases of unknown etiology, comprehensive multi-pathogen screening and NGS testing should be systematically employed to improve diagnostic accuracy. A recent 2021–2022 study conducted in Fujian Province identified 74 psittacosis cases through NGS diagnostics (*7*). However, comprehensive epidemiological investigations and environmental traceability studies for these cases remain notably lacking, representing a significant gap in our understanding of transmission dynamics and environmental reservoirs.

This report documents the first detection and successful identification of *C. psittaci* from environmental samples in Putian City, establishing a valuable reference framework for investigating and managing future psittacosis cases. Upon receiving notification from the medical institution, the Public Health Department immediately coordinated with the Agricultural Department to implement comprehensive control measures. These included the safe disposal of all poultry, thorough disinfection of both the patient's residence and poultry housing facilities, and enhanced surveillance for suspected psittacosis cases throughout the surrounding village. Subsequent investigation revealed that all village poultry were maintained in appropriate housing conditions and displayed no clinical symptoms suggestive of infection.

Conflicts of interest: No conflicts of interest.

Funding: Supported by the Fujian Provincial

Medical Innovation Project (No.2022CXA034) and Fujian Research and Training Grants for Young and Middle-aged Leaders in Healthcare.

doi: 10.46234/ccdcw2025.166

[#] Corresponding author: Fangzhen Xiao, xiaofangzhen@fjcdc.com.cn.

[1] Fujian Center for Disease Control and Prevention, Fujian Provincial Key Laboratory of Zoonosis Research, Fuzhou City, Fujian Province, China; [2] Putian Center for Disease Control and Prevention, Putian City, Fujian Province, China.

Submitted: May 11, 2025
Accepted: July 09, 2025
Issued: July 18, 2025

REFERENCES

1. Zhang ZJ, Zhou H, Cao HE, Ji JK, Zhang RQ, Li WX, et al. Human-to-human transmission of *Chlamydia psittaci* in China, 2020: an epidemiological and aetiological investigation. Lancet Microbe 2022; 3(7):e512 – 20. https://doi.org/10.1016/s2666-5247(22)00064-7.
2. Hou L, Jia J, Qin XC, Fang M, Liang SN, Deng JP, et al. Prevalence and genotypes of *Chlamydia psittaci* in birds and related workers in three cities of China. PLoS One 2024;19(8):e0308532. https://doi.org/10.1371/journal.pone.0308532.
3. Huang WF, Wang FG, Cai QQ, Xu HL, Hong DW, Wu H, et al. Epidemiological and clinical characteristics of psittacosis among cases with complicated or atypical pulmonary infection using metagenomic next-generation sequencing: a multi-center observational study in China. Ann Clin Microbiol Antimicrob 2023;22(1):80. https://doi.org/10.1186/s12941-023-00631-w.
4. Sun Z, Xu K, Huo LL, Zhang XL, Wang Y, Gong YH, et al. Epidemiological features and risk factors of human psittacosis in Hangzhou City, Eastern China. Front Public Health 2025;13:1512841. https://doi.org/10.3389/fpubh.2025.1512841.
5. Shaw KA, Szablewski CM, Kellner S, Kornegay L, Bair P, Brennan S, et al. Psittacosis outbreak among workers at chicken slaughter plants, Virginia and Georgia, USA, 2018. Emerg Infect Dis 2019;25(11):2143 – 5. https://doi.org/10.3201/eid2511.190703.
6. Huang MZ, Wang YF, Lu Y, Qu WX, Zou QD, Zhang D, et al. Clinical characteristics and predicting disease severity in *Chlamydia psittaci* infection based on metagenomic next-generation sequencing. Infect Drug Resist 2025;18:1171 – 81. https://doi.org/10.2147/idr.S509879.
7. Liu KX, Wu LL, Chen GP, Zeng DH, Zhong QW, Luo L, et al. Clinical characteristics of *Chlamydia psittaci* infection diagnosed by metagenomic next-generation sequencing: a retrospective multi-center study in Fujian, China. Infect Drug Resist 2024;17:697 – 708. https://doi.org/10.2147/idr.S443953.

Youth Editorial Board

Indexed by Science Citation Index Expanded (SCIE), Social Sciences Citation Index (SSCI), PubMed Central (PMC), Scopus, Chinese Scientific and Technical Papers and Citations, and Chinese Science Citation Database (CSCD)

The inauguration of *China CDC Weekly* is in part supported by Project for Enhancing International Impact of China STM Journals Category D (PIIJ2-D-04-(2018)) of China Association for Science and Technology (CAST).

CCDC weekly

Vol. 7 No. 29 Jul. 18, 2025

Responsible Authority
National Disease Control and Prevention Administration

Sponsor
Chinese Center for Disease Control and Prevention

Editing and Publishing
China CDC Weekly Editorial Office
No.155 Changbai Road, Changping District, Beijing, China
Tel: 86-10-63150501, 63150701
Email: weekly@chinacdc.cn

CSSN
ISSN 2096-7071 (Print)
ISSN 2096-3101 (Online)
CN 10-1629/R1